agronomy

MDPI

Article

Physiological and Transcriptomic Responses of Two *Rhododendron* L. Cultivars to Drought Stress: Insights into Drought Tolerance Mechanisms

Xueqin Li [1], Xuguang Zheng [2], Yu Wang [3], Songheng Jin [1] and Ziyun Wan [1,*]

[1] Jiyang College, Zhejiang A&F University, Zhuji 311800, China; lxqin@zafu.edu.cn (X.L.); shjin@zafu.edu.cn (S.J.)
[2] Suichang Country Ecological Forestry Development Center, Lishui 323300, China; zheng90909090@sina.com
[3] Zhuji Natural Resources and Planning Bureau, Zhuji 311800, China; way9393@sina.com
* Correspondence: 2020105012012@stu.zafu.edu.cn

Abstract: *Rhododendron* L., a renowned ornamental species and one of the ten famous flowers in China, is highly regarded for its aesthetic value and extensive applications in landscaping. However, its growth and quality are significantly compromised by drought stress, particularly in regions with dry conditions. To elucidate the drought response mechanisms of *Rhododendron*, two cultivars, 'SaKeSiZhiXing' (SKSZX) and 'TuRuiMeiGui' (TRMG), were subjected to natural drought stress, and changes in chlorophyll fluorescence and transcriptomic profiles were examined at 0 days (d), 4 d, and 8 d of drought exposure. An OJIP fluorescence transient (O-J-I-P) analysis revealed a progressive decline in the F_P parameter and an increase in the F_J parameter as drought stress intensified. Additionally, a delayed fluorescence (DF) analysis showed a gradual reduction in the I_1 and I_2 values within the induction and decay curves under prolonged drought conditions. The 820 nm curve indicated the deactivation of a transient phase characterized by a rapid decline, followed by a slow recovery in the modulated reflection (MR) signal. A transcriptomic analysis of leaves identified 24,352, 18,688, and 32,261 differentially expressed genes (DEGs) in SKSZX at 0 d, 4 d, and 8 d of drought treatment, respectively. In contrast, TRMG exhibited more pronounced and earlier drought-induced alterations. These DEGs were primarily enriched in pathways related to phenylpropanoid biosynthesis, plant hormone signaling, photosynthesis, and photosynthesis-antenna proteins. Additionally, 565 transcription factors (TFs) were identified, including bHLH, WRKY, bZIP, MYB-related, MYB, C2H2, and HSF families. The drought-induced changes in TRMG were more substantial and occurred earlier compared to SKSZX, with a greater impairment in the electron transfer capacity at both the donor and acceptor sides of photosystem II (PSII). This study provides valuable insights into the molecular mechanisms underlying drought tolerance in *Rhododendron* and offers a foundation for molecular breeding strategies aimed at enhancing drought resistance in future cultivars.

Keywords: drought stress; *Rhododendron*; chlorophyll fluorescence; transcriptome analysis; transcription factors

check for updates

Academic Editors: Eleni Tani and Eleni Abraham

Received: 15 April 2025
Revised: 20 May 2025
Accepted: 20 May 2025
Published: 23 May 2025

Citation: Li, X.; Zheng, X.; Wang, Y.; Jin, S.; Wan, Z. Physiological and Transcriptomic Responses of Two *Rhododendron* L. Cultivars to Drought Stress: Insights into Drought Tolerance Mechanisms. *Agronomy* **2025**, *15*, 1278. https://doi.org/10.3390/agronomy15061278

Copyright: © 2025 by the authors. Licensee MDPI, Basel, Switzerland. This article is an open access article distributed under the terms and conditions of the Creative Commons Attribution (CC BY) license (https://creativecommons.org/licenses/by/4.0/).

1. Introduction

Rhododendron, a member of the Ericaceae family within the dicotyledonous class, is one of the largest genera of angiosperms in China and is recognized as one of the world's four major floral lineages [1]. Renowned for its striking floral displays, therapeutic and horticultural value, and adaptability to a wide range of environmental conditions, *Rhododendron*

has achieved global dissemination [2–4]. The genus includes over 1000 species and tens of thousands of commercial hybrids, with approximately 650 species endemic to China. The convergence of the Tibetan, Yunnan, and Sichuan provinces forms a crucial center for the dissemination of *Rhododendron* species [5,6]. Since the 18th century, numerous Chinese *Rhododendron* cultivars have been introduced to Europe, particularly to England and Belgium, where they have contributed significantly to ornamental breeding programs [7]. The global economic value of *Rhododendron* cultivation holds significant importance in the horticultural trade. As one of the primary production regions, Zhangping City in Fujian Province, China, achieved an annual sales volume of 10 million potted *Rhododendrons* in 2015, generating a production value of approximately 200 million CNY (RMB), accounting for 70% of the national sales of Belgian azaleas [8,9]. In international markets, Belgium and Denmark produce around 700 million plants annually, while Germany yields 400 million plants [10]. The United States has developed over 5000 hybrid cultivars [11]. Globally, more than 28,000 *Rhododendron* varieties have been registered, making it the second-largest ornamental flower market after roses [12]. Although comprehensive global production value data remain limited, the case of Zhangping and the large-scale production in high-output regions underscore the substantial economic contributions of *Rhododendrons* in ornamental horticulture, particularly in potted flowers, nursery stocks, and high-end bonsai markets [13]. Notably, regional disparities exist: China predominantly focuses on potted flower consumption, whereas European and American markets prioritize landscaping applications and cultivar innovation [14,15]. *Rhododendron* species typically bloom from late spring to early summer; however, select low-maintenance cultivars flower early, around Christmas and during Spring festivals, offering a distinctive floral display when few other plants are in bloom. The growing utilization of *Rhododendron* cultivars in ornamental horticulture, driven by hybridization and cultivation efforts, has established them as preferred choices for potted plants and landscape shrubs in Europe, North America, and Asia [7,16]. Due to their diverse varieties, adaptability and stress resilience, and ease of cultivation and maintenance, *Rhododendron* species are frequently encountered in urban roadways, parks, scenic areas, and other public landscapes [1].

Among various environmental stressors, drought stress poses a significant constraint on plant growth, survival, and productivity [17,18]. The expansion of human populations, global water scarcity, and erratic climate patterns collectively exacerbate the severity of drought conditions. Water deficits disrupt photosynthesis, hinder metabolic processes, reduce CO_2 exchange, and damage chloroplast structures, leading to physiological changes associated with stress responses [19–21]. In response to water scarcity, plants undergo a variety of physiological, cellular, and molecular adaptations to enhance stress tolerance [22]. However, drought stress often inhibits photosynthesis, stunts plant growth, and reduces dry matter accumulation [23,24]. Non-invasive techniques, such as prompt fluorescence (PF), delayed fluorescence (DF), and modulated reflection at 820 nm (MR), have been widely used to assess the photosynthetic electron transport chain and monitor the physiological status of plants under stress conditions. The PF transient is influenced by the redox state of the Photosystem II (PSII) reaction centers (RC), reflecting distinct reduction processes within the electron transport chain [25–28]. DF, initially described by Strehler and Arnold [29], occurs during the light-to-dark transition and represents recombination processes between the reduced primary electron acceptor QA^- and the oxidized donor ($P680^+$) of PSII. Changes in MR at 820 nm reflect variations in the redox states of Photosystem I (PSI) and plastocyanin (PC), with minor contributions from ferredoxin [30].

A wide array of functional and regulatory genes has been identified in relation to drought stress, with fluctuations in the expression of drought-resistant genes significantly advancing our understanding of the molecular mechanisms underlying drought adapta-

tion [22,31–33]. Transcriptomic studies have revealed numerous drought-inducible genes associated with stress responses and resistance [17]. These genes can be broadly categorized into two functional groups: the first includes proteins such as late embryogenesis abundant (LEA) proteins, ROS detoxification enzymes, molecular chaperones, heat shock proteins (HSPs), and lipid-transfer proteins [22,34], while the second group encompasses regulatory proteins or transcription factors (TFs) such as phospholipases and dehydration-responsive elements, which play roles in signal transduction and the regulation of stress-responsive gene expression [35,36]. With the advancement of next-generation sequencing (NGS) technologies, RNA sequencing (RNA-seq) has emerged as a powerful tool for analyzing plant gene expression profiles, especially in the study of drought and salt tolerance [37]. De novo assembly reconstructs transcripts without a reference genome, suitable for non-model organisms but prone to errors or fragmentation. Reference-based assembly aligns reads to a genome, ensuring higher accuracy and isoform detection, but it requires a quality genome [38–40]. The widespread use of RNA-seq for identifying differentially expressed genes (DEGs) under various conditions highlights its utility in providing comprehensive insights into gene expression dynamics across treatments, tissues, and growth stages [37]. Prior to this experiment, we conducted preliminary drought trials on four major commercial *Rhododendron* cultivars. Based on their divergent physiological responses, 'SaKeSiZhiXing' (SKSZX) and 'TuRuiMeiGui' (TRMG) were ultimately selected as the experimental materials. In this study, we employed a multi-functional plant efficiency analyzer (M-PEA, Hansatech, UK) to assess photosynthetic changes and light protection mechanisms in *Rhododendron* under drought conditions. Combined with transcriptomic analysis, this approach allowed us to explore the physiological and molecular responses of *Rhododendron* to water deficits, identify drought-resistant genes, and gain valuable insights into the underlying mechanisms of drought tolerance. These findings contribute to the identification of key genes for future *Rhododendron* breeding programs and enhance our understanding of the molecular responses to drought stress in plants.

2. Materials and Methods

2.1. Plant Material and Drought Treatments

Three-year-old seedlings of *Rhododendron* cultivars 'SaKeSiZhiXing' (SKSZX) and 'TuRuiMeiGui' (TRMG) were obtained from Jiashan United Agricultural Technology Co., Ltd. (Jiaxing, China), a commercial nursery specializing in ornamental plant production. The plants were cultivated in a controlled plant climate incubator (75% humidity, a 14 h light/10 h dark photoperiod, 25 °C day/20 °C night, and 600 μmol m^{-2} s^{-1} light intensity). Soil water content was monitored using a soil temperature and moisture sensor (HSTL-TRSC02, Beijing, China) to maintain 65–70% of the soil's saturated water content. During the one-month adaptation period, uniform-sized plants exhibiting similar growth characteristics were chosen for drought treatments. Drought stress was administered to the experimental groups for 0 d (control), 4 d, 8 d, and 10 d (16–27 July 2023), with all stress-treated groups evaluated against their respective 0 d baselines to quantify drought-induced temporal variations. After each treatment period, leaves were harvested, immediately frozen in liquid nitrogen, and stored at −80 °C for subsequent analyses. Each experimental condition was performed in triplicate.

2.2. Simultaneous Measurement of the Kinetics of PF, DF, and MR

The leaf-level kinetics of OJIP transient, delayed fluorescence (DF), and modulated reflection at 820 nm (MR) were simultaneously measured by a Multi-functional Plant Efficiency Analyser (M-PEA, Hansatech Instruments, Pentney, UK). The second or third fully expanded leaf from the apex was selected for measurement. An actinic LED provided uni-

form illumination with an intensity of 5000 μmol m^{-2} s^{-1}, and the wavelengths used were 627 ± 10 nm for the actinic light, 820 ± 25 nm for the modulated light, and 735 ± 15 nm for the far-red light. An RG long-pass filter was applied to eliminate interference from other light components, and high-quality optical bandpass filters were employed to protect the detectors. Leaves were dark-adapted for 30 min prior to measurement. During data acquisition, the PF and DF measurements were alternated by light and dark intervals for PF and MR in the light and for DF in the dark [41,42]. The following key fluorescence parameters were recorded: minimum fluorescence intensity (F_O) recorded at 20 μs after actinic illumination, maximum fluorescence intensity (F_M) when all PSII reaction centers were closed, and fluorescence intensities at 300 μs (K-step, F_K), 2 ms (J-step, F_J), and 30 ms (I-step, F_I).

Several parameters were derived from the OJIP transients based on established methods [41,43,44], including the maximum quantum yield of PSII (F_V/F_M), the quantum efficiency of energy dissipation at t = F_O (φD_O), the quantum efficiency of energy dissipation at t = F_O (φE_O), the trapped exciton that moves an electron into the electron transport chain beyond Q_A^- (ψ_O), the performance index for energy conservation from exciton to the reduction of PSI terminal acceptors (PI_{TOTAL}), the performance index on an absorption basis (PI_{ABS}), the efficiency of an electron beyond that reduced PSI acceptors (δR_O), the ABS per cross-sectional area (CS) at t = F_M (ABS/CS_M), the trapped energy flux per CS at t = F_M (TR_O/CS_M), the dissipated energy flux per CS at t = F_M (DI_O/CS_M), the electron flux per CS at t = F_M (ET_O/CS_M), and the electron transport flux per CS at t = F_M (RE_O/CS_M).

2.3. Total RNA Isolation and Transcriptome Sequencing

Total RNA was extracted from both control and drought-treated leaves using the RNAprep Pure Polysaccharides & Polyphenolics-rich Plant Kit (DP441, TianGen, Beijing, BJ, China), following the manufacturer's protocol. RNA integrity and quantity were assessed using the RNA Nano 6000 Assay Kit on the Bioanalyzer 2100 system (Agilent Technologies, Santa Clara, CA, USA).

Transcriptome sequencing was conducted by Beijing Novogene Biotechnology Co., Ltd. (Beijing, China). Briefly, Poly (A) mRNA was isolated using poly-T oligo (dT) magnetic beads. Fragmentation was carried out in first-strand synthesis reaction buffer (5X) using divalent cations at elevated temperatures. Taking these short mRNA fragments as templates, random hexamer-primers were used to create the first-strand cDNA, and RNaseH and DNA polymerase I were then used to produce the second-strand cDNA. The purified double-stranded cDNA was then coupled to sequencing adaptors following end repair and poly (A) addition. Purified library fragments were screened with the AMPure XP system (Beckman Coulter, Beverly, CA, USA) to screen cDNA fragments of preferentially 370–420 bp. The PCR products were then purified using AMPure XP beads. To ensure the quality of the library, the library was initially quantified with a Qubit2.0 fluorometer, then qualified with an Agilent 2100 bioanalyzer. Finally, the cDNA libraries were sequenced on an Illumina NovaSeq 6000 platform (Illumina, San Diego, CA, USA).

Raw data (raw reads) were first processed using in-house Perl scripts. Clean data (clean reads) were obtained in this step by removing adapter reads, N base reads, and low-quality reads from raw data. At the same time, the clean data's Q20, Q30, and GC content were calculated. All subsequent analyses were based on clean, high-quality data.

2.4. De Novo Transcriptome Assembly and Functional Annotation

A de novo transcriptome assembly approach using Trinity v2.6.6 (with min_kmer_cov set to 2 by default and all other parameters set to default) was undertaken due to the absence of a high-quality, annotated reference genome for *Rhododendron* L. at the time

of analysis. All assembled clean data were aligned to transcripts using RSEM (v1.2.15) with the default settings. The sequence assembled by Trinity was known as a transcript. Furthermore, all clean reads were mapped to the transcripts. The completeness of the assembled transcriptome was assessed using BUSCO software (v3.0.2). For functional annotation, the assembled sequences were aligned to public databases, including Nr (NCBI non-redundant protein sequences), Nt (NCBI non-redundant nucleotide sequences), Pfam (Protein family), KOG/COG (Clusters of Orthologous Groups of proteins), Swiss-Prot (A manually annotated and reviewed protein sequence database), KEGG (Kyoto Encyclopedia of Genes and Genomes database), and GO (Gene Ontology).

2.5. Differential Gene Expression Analysis

DEG analysis was estimated using the DESeq2 R package (v1.20.0), with adjustments to *p*-values using Benjamini and Hochberg's method to control the false discovery rate. A threshold of *p*adj < 0.05 and $|\log2\ (\text{foldchange})| > 1$ was set to determine significant differential expression. GO enrichment analysis was conducted using the GOseq package (v1.10.0) based on the Wallenius non-central hypergeometric distribution. KEGG pathway enrichment of DEGs was conducted using KOBAS (v2.0.12) software. Results were visualized using BioRender online software (https://www.biorender.com/ (accessed on 14 May 2024)).

2.6. Gene Validation of RNA-Seq by qRT-PCR Analysis

To validate the expression profiles of DEGs, quantitative real-time PCR (qRT-PCR) analysis was conducted on a LightCycler® 480 II (Roche Diagnostics, Mannheim, BW, Germany), following the manufacturer's protocols. Gene-specific primers were designed using Primer Premier 5.0, with Glyceraldehyde 3-phosphate dehydrogenase (*GAPDH*) as the internal control gene. Information on the primer sequence is provided in Table S1. Total RNA from leaves subjected to different drought stress conditions was extracted using FastPure Plant Total RNA Isolation Kit (Polysaccharides& Polyphenolics-rich) (Vazyme, Nanjing, China); then, first-strand cDNA was synthesized from 1 μg of total RNA using the HiScript III All-in-one RT SuperMix Perfect for qPCR (Vazyme). Subsequently, the diluted cDNA was used as the template for qRT-PCR with 2 × ChamQ Universal SYBR qPCR Master Mix. The PCR amplification was conducted in a volume of 10 μL, containing 5 μL of 2 × Master Mix, 0.2 μL of each primer, 2 μL of cDNA, and 2.6 μL of deionized water. The reaction conditions for all samples were as follows: initial denaturation at 95 °C for 30 s, followed by 40 cycles of 95 °C for 10 s, 60 °C for 30 s, and 72 °C for 30 s. The relative expression level of genes was calculated using the $2^{-\Delta\Delta CT}$ method, with three technical replicates for each sample.

2.7. Statistical Analysis

All experimental data were analyzed using Microsoft Excel 2010 and SPSS v20.0 software (IBM Corporation, Armonk, NY, USA). The Duncan test was used to compare significant difference among all samples ($p < 0.05$).

3. Results

3.1. Comparative Analysis of Morphological and Chlorophyll Fluorescence of Responses of Rhododendron Cultivars Under Drought Stress

Drought stress significantly affected the morphology and chlorophyll fluorescence of two *Rhododendron* cultivars, with varying degrees of response observed. Under normal watering conditions, no substantial morphological changes were evident in either of the two *Rhododendron* cultivars (Figure S1A,D). However, SKSZX displayed only mild stress symptoms during drought treatment (Figure S1B,C), while TRMG exhibited severe stress

responses, including leaf curling, drooping, yellowing, and wilting, which were apparent at as early as 4 and 8 d of drought stress (Figure S1E,F). The water deficit significantly impaired photosynthesis, a critical process for plant growth and development. To investigate the photosynthetic responses under drought stress, a multi-functional plant efficiency analyzer (M-PEA) was employed to assess PF, DF induction, and MR kinetics. In both cultivars, F_O increased, while F_P gradually decreased progressively with prolonged drought stress (Figure 1A,D). The I-P amplitude of the OJIP transient decreased in parallel with the decline in F_P, particularly at the later stages of drought treatment. Upon normalizing the transients between F_O and F_P, the J step of TRMG was noticeably higher at 8 d of dehydration stress, whereas SKSZX did not exhibit significant alterations until 10 d of drought exposure (Figure 1B,E). Furthermore, under drought stress, the J step of the PF transients was markedly higher than in the control group. The ΔJ values increased with the duration of drought treatment, reaching 0.12 in SKSZX (Figure 1C). In comparison to SKSZX, TRMG exhibited a more pronounced and rapid increase in ΔJ (Figure 1F).

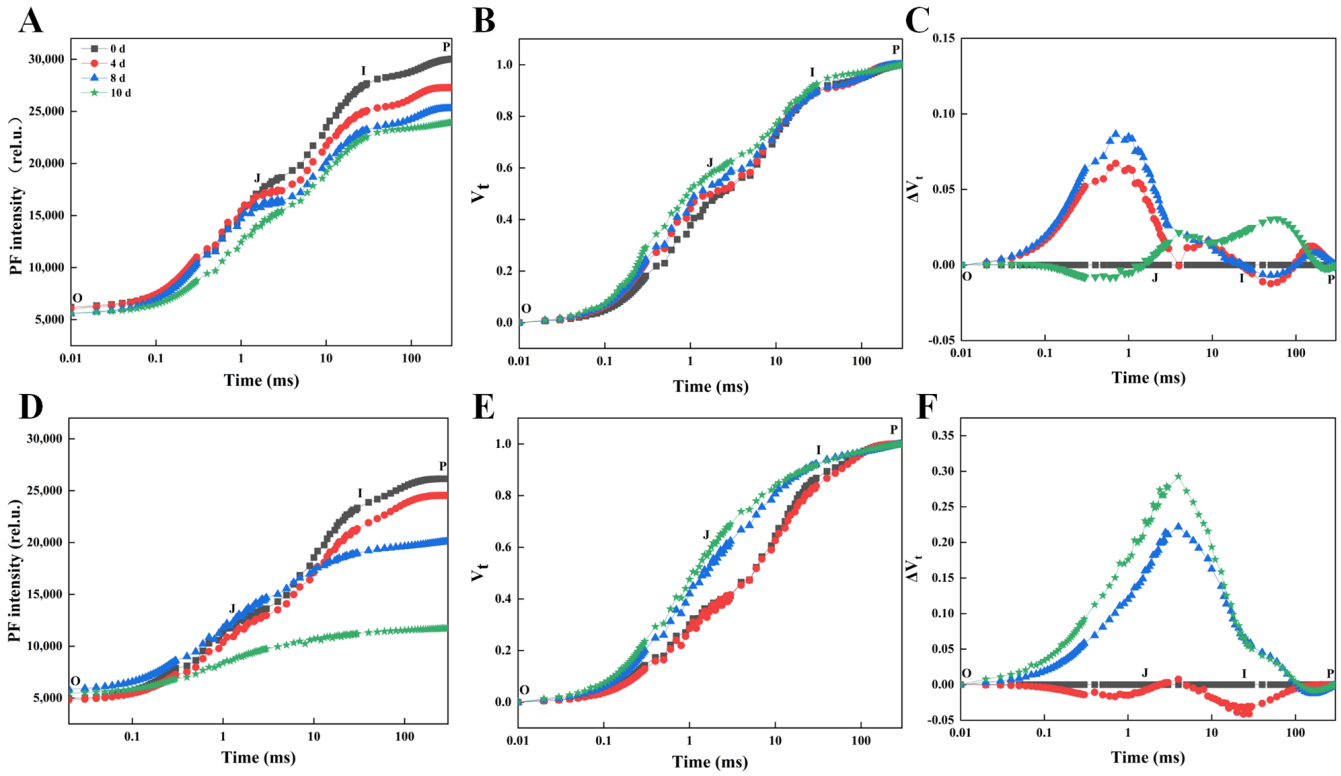


Figure 1. The prompt fluorescence transients of the two cultivars SKSZX and TRMG on 0 d, 4 d, 8 d, and 10 d of drought treatment. (**A**–**C**) Absolute values, normalized transients, and ΔV_t curves of SKSZX. (**D**–**F**) Absolute values, normalized transients, and ΔV_t curves of TRMG. The signals were plotted on a logarithmic time scale. Note: O point represents baseline fluorescence (F_0) before the start of illumination (time t = 0); J point corresponds to the first reduction of QA (primary electron acceptor of PSII); I point reflects further QA^- accumulation and involvement of the plastoquinone (PQ) pool; P point represents maximum fluorescence (F_m) when QA is fully reduced (PSII centers closed).

The redox states of P700 and PC are reflected in the typical 820 nm kinetics, which consist of a decreasing phase, followed by an increasing phase. The decreasing phase represents the oxidation of PSI and PC, while the increasing phase corresponds to their reduction. The oxidation and reduction rates of PC and PSI are equivalent to their reduction rates when the 820 nm kinetics reaches its lowest point [41]. During drought treatment, both cultivars showed a distinct change in their MR/MR_O kinetics curves, with the lowest points occurring later as the severity of drought stress increased. Notably, no significant change

in the oxidation rate (represented by the steepest drop in the MR/MR_O transient) was observed between the treated and control groups for either cultivar (Figure 2A,D). However, after 10 d of drought treatment, the reduction rate in TRMG significantly decreased. DF induction curves were constructed by measuring the signals at a specific dark time-point of 20 µs within each dark interval. The DF intensity increased from an initial minimum (D_0) to a peak (I_1) at 3 ms, followed by a plateau (I_2) at approximately 100 ms (Figure 2B,E). As drought stress intensified, the I_1 value gradually decreased, whereas no significant change was observed at the maximum I_2. The DF decay kinetics at I_1 in TRMG leaves showed a rapid decrease, which was significantly greater than that observed in SKSZX (Figure 2C,F).

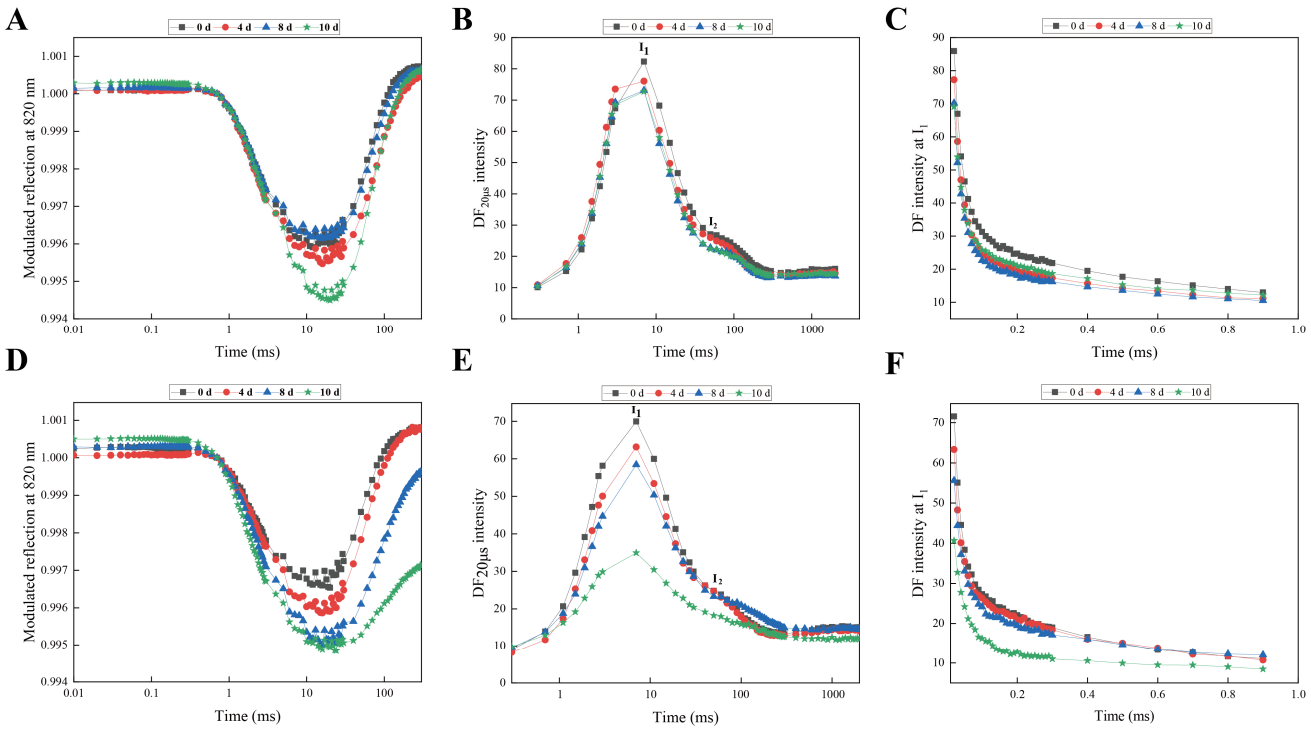


Figure 2. The MR and DF kinetics in the leaves of SKSZX and TRMG. (**A**–**C**), (**D**–**F**) Modulated 820 nm reflection (MR/MR_O), delayed chlorophyll a fluorescence, and decay kinetics of DF at the maxima I_1 (7 ms) in SKSZX and TRMG, respectively. The first two signals were plotted on a logarithmic time scale, while the decay kinetics are presented on a linear time scale. Each curve represents the average of three replicates.

The PF parameters in *Rhododendron* leaves were significantly influenced by both cultivars and the severity of drought stress (Figure 3). Under drought treatment, metrics such as F_V/F_M, φE_O, ψ_O, PI_{TOTAL}, and PI_{ABS} all decreased in both cultivars, whereas δR_O and φD_O exhibited clear increases. TRMG showed more rapid declines in these metrics compared to SKSZX. Additionally, SKSZX maintained higher values of F_V/F_M, φE_O, ψ_O, PI_{TOTAL}, and PI_{ABS} after 10 d of water deficit. The absorbed energy fluxes are shown in Figure 3H–L, with the exception of DI_O/CS_M, ABS/CS_M, TR_O/CS_M, ET_O/CS_M, and RE_O/CS_M, all of which decreased in response to drought stress. Notably, SKSZX experienced a slower decrease in these four metrics compared to TRMG.

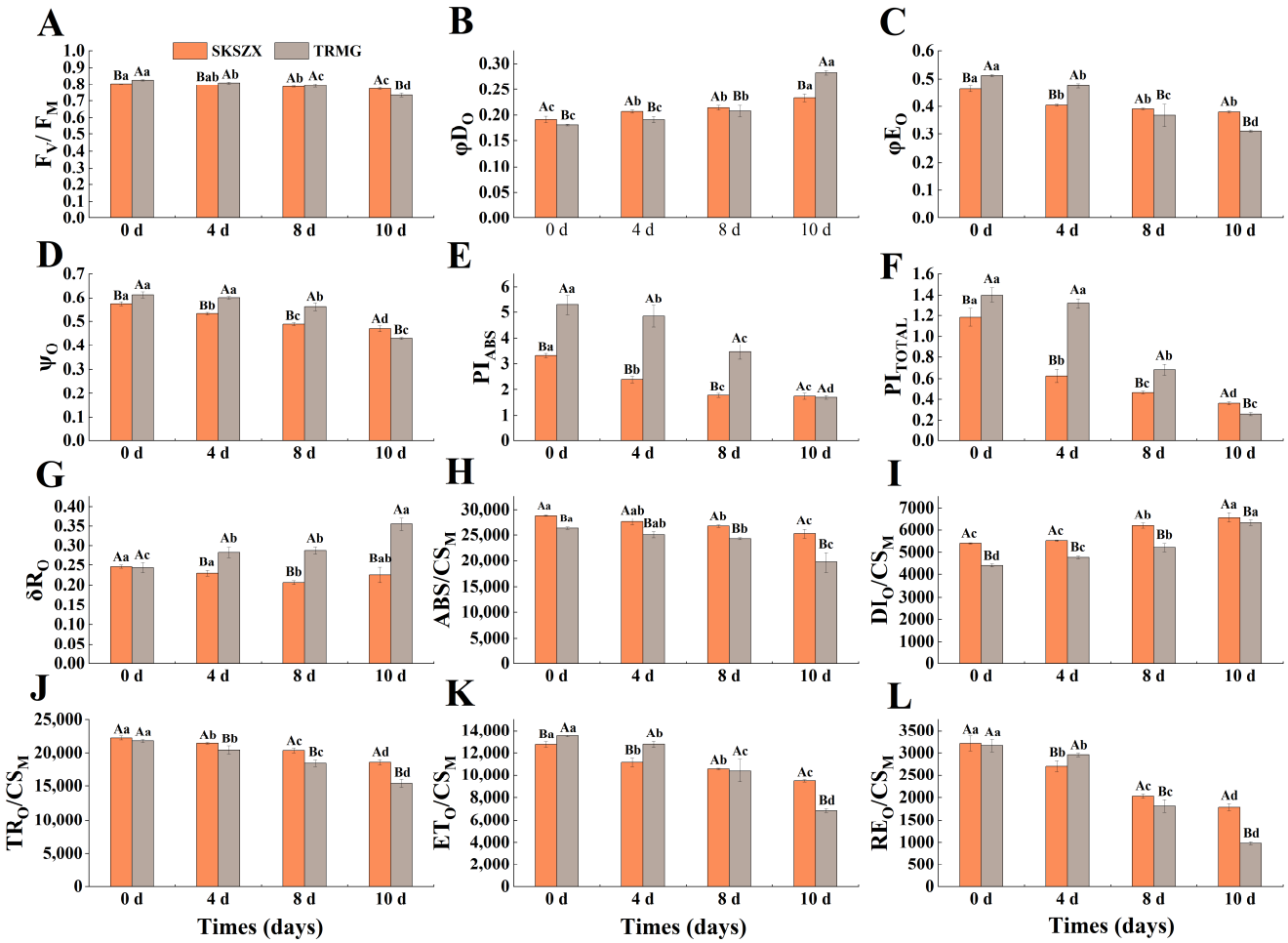


Figure 3. Parameters derived from the prompt chlorophyll a fluorescence transients in leaves of SKSZX and TRMG. (**A**) The maximum photochemical efficiency of PSl (F_V/F_M). (**B**) The quantum efficiencyof energy dissipation (φD_O). (**C**) The quantum yield for electron transport (φE_O). (**D**) The probability that an electron moves further than QA^- (ψ_O). (**E**) The performance index on an absorption basis (PI_{ABS}). (**F**) Total performance index of the photosynthetic apparatus (PI_{TOTAL}). (**G**) The efficiency of an electron beyond QA^- that reduced PSI acceptors (δR_O). (**H**) Absorption per cross-sectional area of the photosynthetic apparatus (ABS/CS_M). (**I**) Dissipation of excitation energy per cross-sectional area (DI_O/CS_M). (**J**) The rate of primary photochemical capture per unit cross-sectional area (TR_O/CS_M). (**K**) Electron transport rate per unit area (ET_O/CS_M). (**L**) Relative variable energy quantum yield of electron transport (RE_O/CS_M). All data represent the standard deviation of three repetitions; each repetition contains 3 seedlings. Different capital letters indicate significant differences between cultivars, while different lowercase letters indicate significant differences between treatments.

3.2. Illumina Sequencing and De Novo Assembly

To identify drought-responsive unigenes in SKSZX and TRMG, RNA-seq analysis was performed using the Illumina NovaSeq 6000 platform. The transcriptomic sequencing data for 18 samples demonstrated high quality and robust preprocessing outcomes, as summarized in Table 1. Raw sequencing reads ranged from 19.89 million (S0_2) to 22.32 million (T4_2), yielding raw bases between 5.97 Gb (S0_2) and 6.70 Gb (T4_2). After stringent quality control, 96.7–97.5% of raw reads were retained as clean reads, corresponding to clean bases of 6.07–6.61 Gb, indicating minimal data loss during adapter trimming and low-quality sequence removal. Sequencing accuracy, assessed by Q20 (percentage of bases with Phred score $\geq$ 20) and Q30 (Phred score $\geq$ 30), exceeded standard thresholds for RNA-seq analysis. Q20 (>96.7%) and Q30 (>91.3%) exceeded standard thresholds,

with the highest Q30 observed in T4_1 (93.01%). The GC content remained stable across samples (46.19–47.41%), consistent with typical plant transcriptomes and indicative of negligible contamination or sequencing bias. The efficiency of the assembly process achieved completeness levels of 71.22–74.59%, as assessed by BUSCO software. This reflects the moderate assembly rates expected when working with non-model species that lack a complete reference genome. Transcriptomic profiling revealed that different drought stress treatments significantly altered the gene expression in *Rhododendron* leaves (Figure S2A). To assess the reproducibility of the sequencing data, a correlation analysis was conducted using fragments per kilobase of exon per million fragments mapped (FPKM) values. The results showed a high degree of consistency among the three biological replicates, with Pearson's correlation coefficients ranging from 0.808 to 0.923 (Figure S2B). Furthermore, a principal component analysis (PCA) clearly separated SKSZX and TRMG, indicating good repeatability within each cultivar group (Figure S2C).

Table 1. The transcriptome sequencing statistics of 18 libraries.

Sample	Raw Reads	Raw Bases	Clean Reads	Clean Bases	Q20	Q30	GC%	Total Mapped
T0_1	21,348,835	6.40 G	21,119,862	6.34 G	97.36	92.78	46.50	15,489,054 (73.34%)
T0_2	20,665,066	6.20 G	20,492,396	6.15 G	97.13	92.22	47.08	15,222,784 (74.29%)
T0_3	21,496,496	6.45 G	21,256,541	6.38 G	97.32	92.66	47.00	15,611,864 (73.44%)
T4_1	21,410,582	6.42 G	20,975,564	6.29 G	97.46	93.01	46.70	15,471,085 (73.76%)
T4_2	22,322,178	6.70 G	22,018,751	6.61 G	97.30	92.56	47.06	16,301,578 (74.03%)
T4_3	20,940,896	6.28 G	20,701,885	6.21 G	97.10	92.16	46.54	15,441,596 (74.59%)
T8_1	21,688,245	6.51 G	21,363,087	6.41 G	96.84	91.62	46.56	15,646,965 (73.24%)
T8_2	22,029,407	6.61 G	21,801,613	6.54 G	96.97	91.9	46.19	15,731,135 (72.16%)
T8_3	22,015,159	6.60 G	21,759,277	6.53 G	97.16	92.35	46.25	15,839,005 (72.79%)
S0_1	22,043,155	6.61 G	21,519,281	6.46 G	97.12	92.19	46.33	15,635,255 (72.66%)
S0_2	19,892,516	5.97 G	19,596,253	5.88 G	96.99	92.02	46.54	14,005,860 (71.47%)
S0_3	21,969,798	6.59 G	21,589,241	6.48 G	96.70	91.30	46.56	15,376,810 (71.22%)
S4_1	21,774,077	6.53 G	21,492,096	6.45 G	97.38	92.78	46.82	15,554,786 (72.37%)
S4_2	20,938,283	6.28 G	20,469,741	6.14 G	97.23	92.47	47.41	14,817,884 (72.39%)
S4_3	21,065,427	6.32 G	20,693,989	6.21 G	97.19	92.36	47.29	15,136,408 (73.14%)
S8_1	21,221,783	6.37 G	20,927,707	6.28 G	97.10	92.24	46.75	15,142,624 (72.36%)
S8_2	20,830,406	6.25 G	20,624,696	6.19 G	97.14	92.25	46.69	15,037,787 (72.91%)
S8_3	20,394,267	6.12 G	20,218,889	6.07 G	97.15	92.29	46.89	14,725,314 (72.83%)

3.3. Comparisons of DEGs Under the Different Drought Stress Stages

We compared the DEGs in *Rhododendron* leaves from SKSZX and TRMG at different drought stress stages (0 d, 4 d, and 8 d). A total of 24,352, 18,688, and 32,261 DEGs were identified in the comparisons between S_0 d vs. T_0 d, S_4 d vs. T_4 d, and S_8 d vs. T_8 d, respectively (Figure 4A). Additionally, 1710 DEGs (including 971 downregulated and 739 upregulated genes) and 8144 DEGs (including 3050 downregulated and 5094 upregulated genes) were observed between S_0 d vs. S_4 d and S_0 d vs. S_8 d, respectively. Similarly, 3283 DEGs (including 1191 downregulated and 2092 upregulated genes) and 19,642 DEGs (including 10,242 downregulated and 9400 upregulated genes) were obtained in T_0 d vs. T_4 d and T_0 d vs. T_8 d. The number of DEGs increased with prolonged drought stress, suggesting that the majority of drought-responsive genes were activated relatively late in the stress period. Notably, the number of DEGs in TRMG was 1.9 and 2.4 times higher than in SKSZX after 4 d and 8 d of drought stress, respectively. These results suggested that gene regulation in TRMG was more pronounced than in SKSZX under drought stress. A Venn diagram of the DEGs revealed that 7573 DEGs were shared between the two cultivars (Figure 4B). Upon comparing the differences between cultivars,

we identified 307 and 10,309 genes that were specifically expressed in TRMG at 4 d and 8 d of drought stress, respectively, whereas 138 and 2765 genes were uniquely expressed in SKSZX. Importantly, 42 DEGs were commonly regulated in both cultivars (Figure 4C).

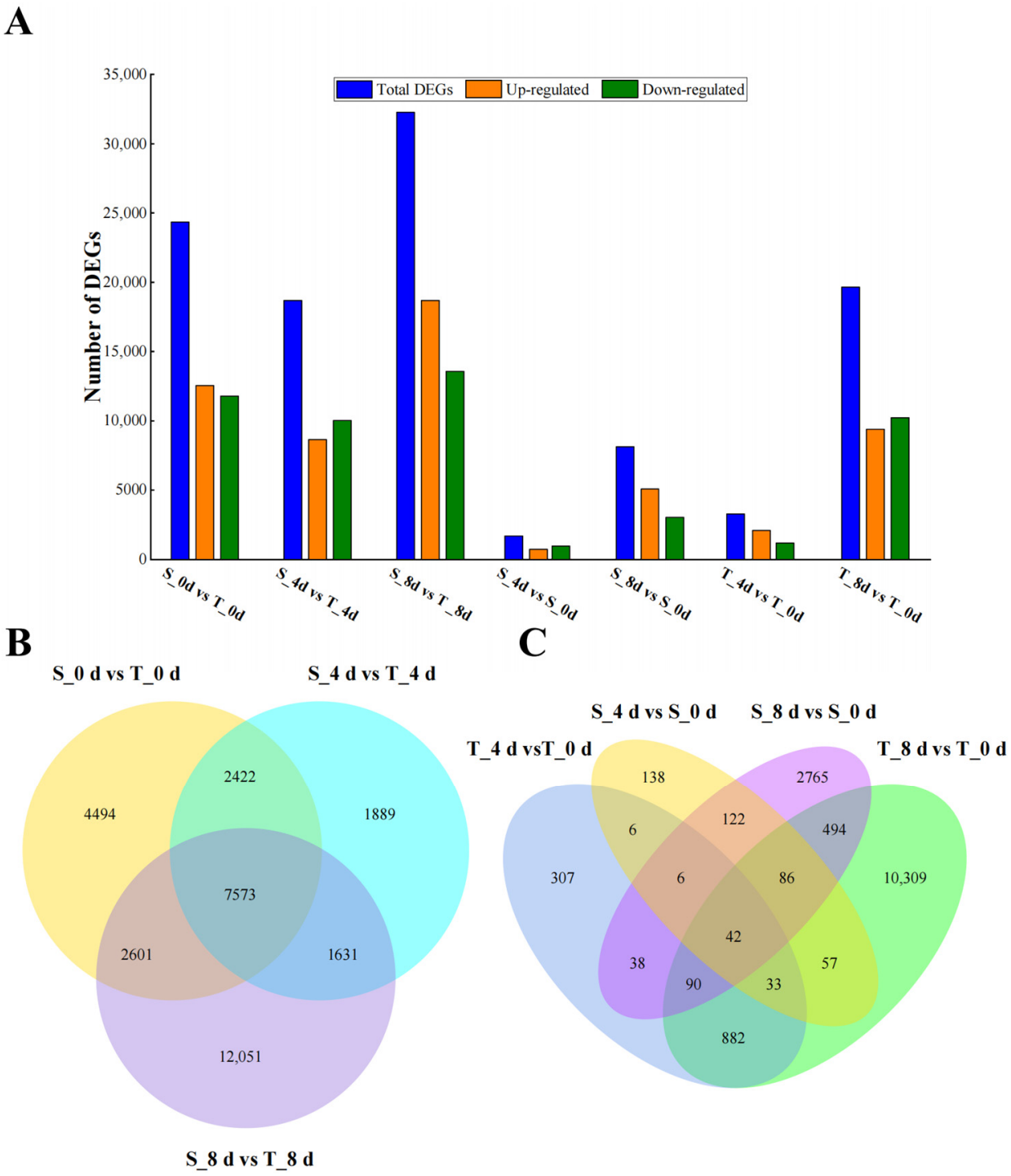


Figure 4. Analysis of differentially expressed genes among two *Rhododendron* species. (**A**) The number of upregulated and downregulated genes in SKSZX (S) and TRMG (T) under drought stress treatment. (**B**) Venn diagram shows the number of DEGs among comparisons of S_0 d vs. T_0 d, S_4 d vs. T_4 d, and S_8 d vs. T_8 d. (**C**) Venn diagram shows the comparison of DEGs between the two *Rhododendron* cultivars under drought stress for 4 d and 8 d.

3.4. GO and KEGG Enrichments of DEGs

To investigate the molecular mechanisms underlying the drought response in the two *Rhododendron* cultivars, Gene Ontology (GO) and Kyoto Encyclopedia of Genes (KEGG) enrichment analyses were performed on the DEGs identified in pairwise comparisons across various drought stress stages. DEGs were categorized into three main GO ontologies, molecular function (MF), biological process (BP), and cellular component (CC). The upregulated DEGs in the comparisons between S_0 d vs. T_0 d and T_4 d vs. S_4 d were primarily enriched in "endoribonuclease activity" (GO:0004521), "ribonuclease activity" (GO:0004540), and "endonuclease activity" (GO:0004519). Surprisingly, the GO analysis of T_8 d vs. S_8 d primarily focused on terms related to 'phosphorylation' (GO:0016310), 'phosphate-containing compound metabolic process' (GO:0006796), 'phosphorus metabolic process' (GO:0006793), 'photosystem II oxygen evolving complex' (GO:0009654), and 'photosystem' (GO: 0009521). The analysis of upregulated and downregulated DEGs revealed significant enrichment in two main GO categories: 'BP' and 'MF'. The most enriched terms included 'binding', 'metabolic process', and 'cell wall' (Table S2), suggesting that genes involved in these processes may be suppressed as a result of dehydration.

A KEGG enrichment analysis revealed that DEGs in the three comparisons (S_0 d vs. T_0 d, S_4 d vs. T_4 d, and S_8 d vs. T_8 d) were enriched in 117, 116, and 121 pathways, respectively (Table S3). Notably, the DEGs in the comparisons between T_4 d vs. T_0 d and T_8 d vs. T_0 d were enriched in 61 and 115 KEGG pathways, respectively, while fewer pathways were enriched in the comparisons between S_4 d vs. S_0 d and S_8 d vs. S_0 d, suggesting that drought stress had a more moderate effect on SKSZX. Among the seven comparative groups, the commonly upregulated genes were significantly enriched in 38 KEGG pathways. Notably, a substantial number of genes were enriched in multiple pathways including Ribosome (ko03010), plant hormone signal transduction (ko04075), starch and sucrose metabolism (ko00500), plant–pathogen interaction (ko04016), and protein processing in the endoplasmic reticulum (ko04141), indicating that drought stress activates these signaling pathways (Figure 5A). In addition, the downregulated genes across the seven comparative groups were collectively enriched in 34 KEGG pathways. Among these, the plant–pathogen interaction pathway (ko04016), protein processing in the endoplasmic reticulum (ko04141), starch and sucrose metabolism (ko00500), and plant hormone signal transduction (ko04075) contained the highest number of genes. Significant gene enrichment was also observed in the photosynthesis (ko00195) and circadian rhythm in plants (ko04712) pathways (Figure 5B). These findings suggested that metabolic and photosynthetic processes may play a predominant role during the later stages of drought treatment. The scatter plots (Figure 5C–F) in the figure illustrate the results of the pathway enrichment analysis for differentially expressed genes (DEGs) under various treatment conditions. The scatter plots (Figure 5C–F) in the figure illustrate the results of the pathway enrichment analysis for up-/downregulated DEGs above the T_8 d vs. T_0 d and S_8 d vs. T_8 d comparative groups. Pathways such as 'Tyrosine metabolism', 'Starch and sucrose metabolism', and 'Plant hormone signal transduction' show a higher significant enrichment (Figure 5C,E). Similarly, they highlight pathways like 'Galactose metabolism' and 'Glycerophospholipid metabolism' that are significantly enriched in downregulated DEGs (Figure 5D,F). The analysis indicates that specific metabolic pathways are differentially affected by drought stress in *Rhododendron*, with certain pathways being upregulated and others downregulated.

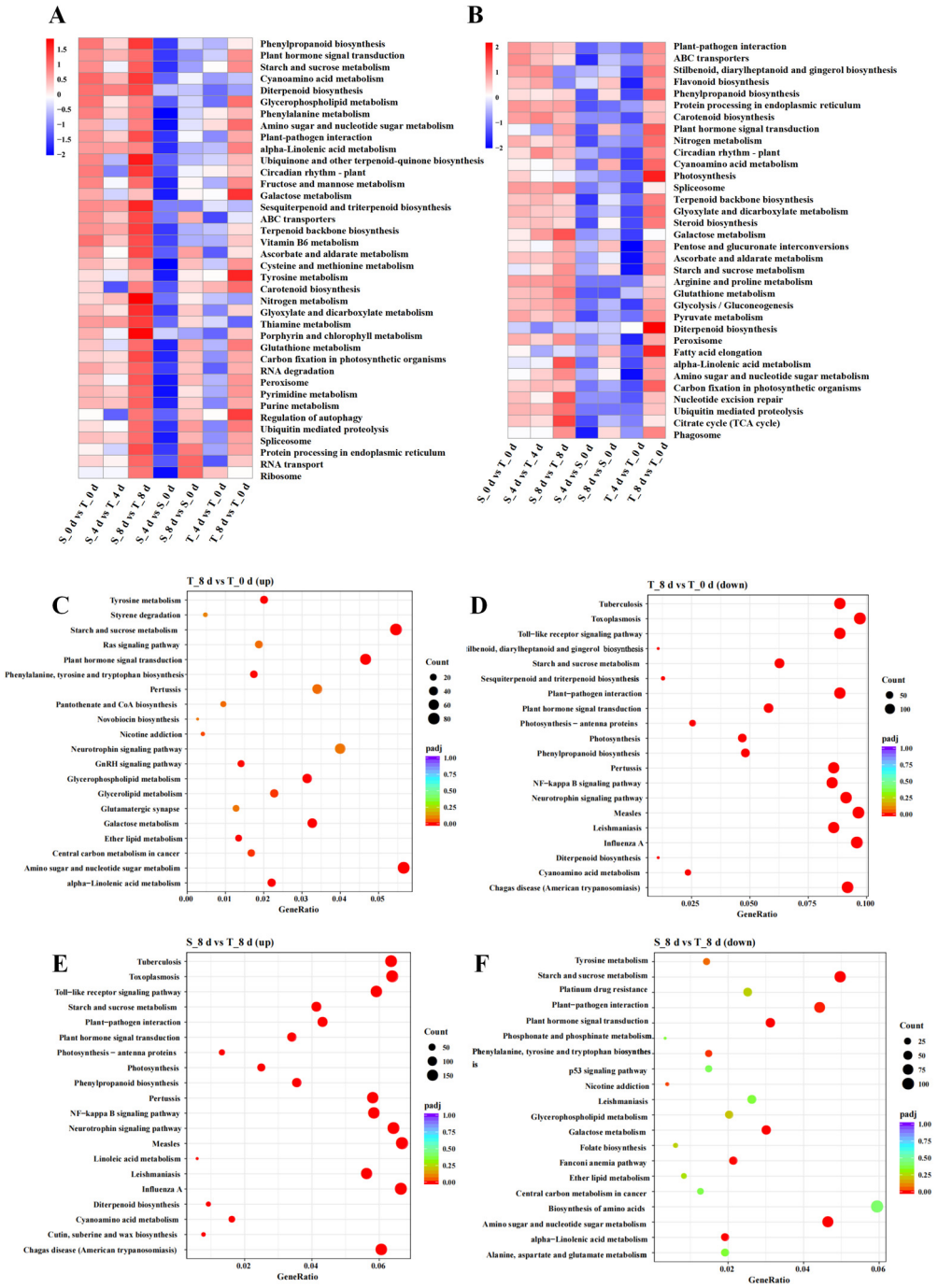


Figure 5. KEGG pathway-enrichment analysis (**A**,**B**) The heat maps of the KEGG pathways co-enriched by up-/downregulated DEGs in the seven comparison groups. (**C**,**D**) Pathway functional enrichment of up-/downregulated DEGs from comparisons of T_8 d vs. T_0 d. (**E**,**F**) Pathway functional enrichment of up-/downregulated DEGs from comparisons of S_8 d vs. T_8 d.

3.5. Identification of Plant Hormone and Signal-Transduction-Related DEGs

Drought stress significantly influenced plant hormone signal transduction, as evidenced by the GO and KEGG enrichment analyses. Specifically, the auxin and abscisic acid (ABA) pathways were found to be involved in the drought response of both cultivars. A total of 22 DEGs were identified in the auxin signaling pathway, exhibiting significant changes in both TRMG and SKSZX (Figure 6A). For instance, four genes encoding AUX1 were downregulated in TRMG after 8 d of drought treatment. Additionally, two genes encoding the auxin-inducing protein AUX/IAA were specifically upregulated, while four genes were

downregulated under the same conditions. The expression of four genes encoding *ARF* was inhibited at 4 d and 8 d, with Cluster-56713.66945 showing a sharp decrease after 8 d of TRMG treatment. One upregulated gene encoding *GH3* and two upregulated genes encoding *SAUR* were found after 4 d of treatment, while two downregulated genes encoding *GH3* and three downregulated genes encoding *SAUR* were observed after 8 d. Furthermore, drought stress also induced the expression of 17 DEGs associated with the ABA-mediated signaling system (Figure 6B). Four genes encoding *PP2C*, a negative regulator of ABA signaling, were downregulated at both 4 and 8 d in TRMG compared to SKSZX. The decreased PP2C activity led to a differential expression of protein kinase *SnRK2* in both cultivars. Specifically, two genes (Cluster-56713.52170 and Cluster-56713.46758) exhibited continuous upregulation, while two genes (Cluster-56713.46511 and Cluster-56713.29308) were continuously downregulated after 8 d of SKSZX treatment. Notably, Cluster-56713.52170 (*SnRK2.4* homolog) and Cluster-56713.46758 (*SnRK2.6* homolog) are strong candidates for further functional validation, as SnRK2 kinases are central regulators of ABA signaling and drought tolerance in plants. Additionally, Cluster-56713.71630 (*ABF3*-like) and Cluster-56713.71875 (*ABF4*-like), which were upregulated in TRMG, may contribute to cultivar-specific stress adaptation. These genes are proposed as priority candidates for future studies on *Rhododendron* drought tolerance mechanisms. Three genes encoding ABA response transcription factors (*ABFs*) were activated, with Cluster-56713.71875 and Cluster-56713.71630 showing a more than two-fold upregulation at T_8 d. In SKSZX, the expression level of Cluster-56713.71875 decreased by 43%, while Cluster-56713.71630 showed no significant change.

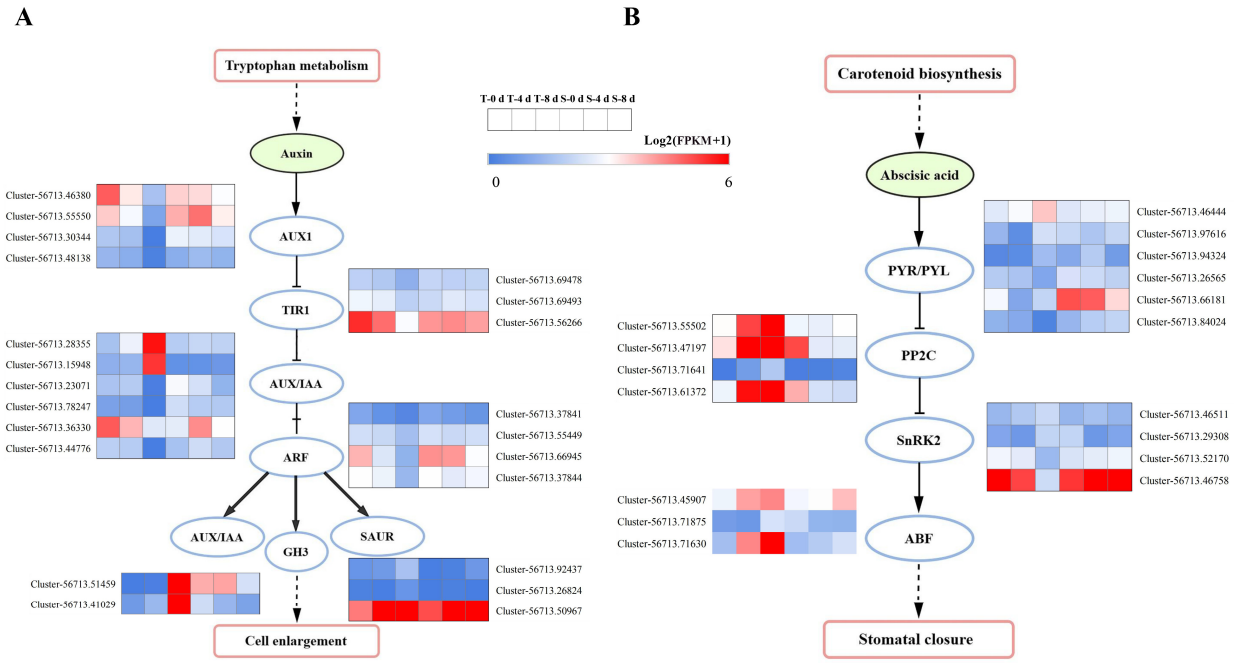


Figure 6. Analysis of auxin (**A**) and abscisic acid (**B**) signaling pathways of DEGs under drought stress.

3.6. Photosynthesis-Related Genes Under Drought Stress

Several DEGs were enriched in the photosynthesis pathway (ko00195) following drought stress treatment. In this study, a total of 31 photosynthesis-related DEGs were identified (Figure 7). Twelve DEGs encoding core components of PSI, including *PsaA*, *PsaB*, *PsaD*, *PsaH*, *PsaK*, and *PsaO*, were strongly downregulated at T-8 d, whereas only a slight downregulation was observed at S_8 d. The expression of photosynthesis-related genes *PsaA* (Cluster-56713.50913, Cluster-56713.50904, and Cluster-56713.50905), *PsaB* (Cluster-56713.65991 and Cluster-56713.53907), and *PsaD* (Cluster-56713.48019 and

Cluster-56713.48018) was significantly downregulated in TRMG at 8 d (T_8 d), with reductions of 52.7%, 77.9%, and 68.3% (*PsaA*); 54.5% and 34.2% (*PsaB*); and 94.0% and 41.2% (*PsaD*), respectively. In contrast, SKSZX exhibited a markedly milder suppression for these genes at S_8 d: Cluster-56713.50904 (13.8%), Cluster-56713.65991 (6.3%), Cluster-56713.53907 (2.4%), Cluster-56713.48019 (34.9%), and Cluster-56713.48018 (14.2%). Additionally, nineteen DEGs encoding key components of PSII, such as *PsbA*, *PsbP*, *PsbR*, *PsbQ*, *PsbS*, *PsbO*, *PetE*, *PetH*, *PetA*, and *PetJ*, exhibited similar expression patterns to PSI-related genes. For instance, key photosynthetic genes including *PsbR* (Cluster-56713.55172), *PetE* (Cluster-56713.56597), *PetH* (Cluster-56713.48018 and Cluster-56713.56552), and *PsbO* (Cluster-56713.50758) exhibited significant downregulation in TRMG at 8 d (T_8 d), with expression reductions of 34.0%, 44.6%, 41.2%, 28.4%, and 32.2%, respectively. In contrast, these genes displayed minimal expression changes or even a slight upregulation in SKSZX at 8 d (S_8 d). Notably, Cluster-56713.55172 and Cluster-56713.56552 were upregulated by 1.7% and 3.8%, respectively, further highlighting the transcriptional resilience of photosynthesis-related components in SKSZX under prolonged drought stress. Notably, key electron transport genes encoding *PetE* (Cluster-56713.48018, Cluster-56713.56552, and Cluster-56713.48019) exhibited cultivar-specific expression patterns under drought stress. In TRMG at 8 d (T_8 d), these genes were significantly downregulated by 41.1%, 28.4%, and 94.0%, respectively. In contrast, SKSZX showed a milder suppression for Cluster-56713.48018 (14.2% downregulation) and Cluster-56713.48019 (34.9% downregulation), while Cluster-56713.56552 was upregulated by 3.8%. These results suggest that drought stress significantly suppressed the expression of genes associated with both PSI and PSII during the middle and later stages of the experiment.

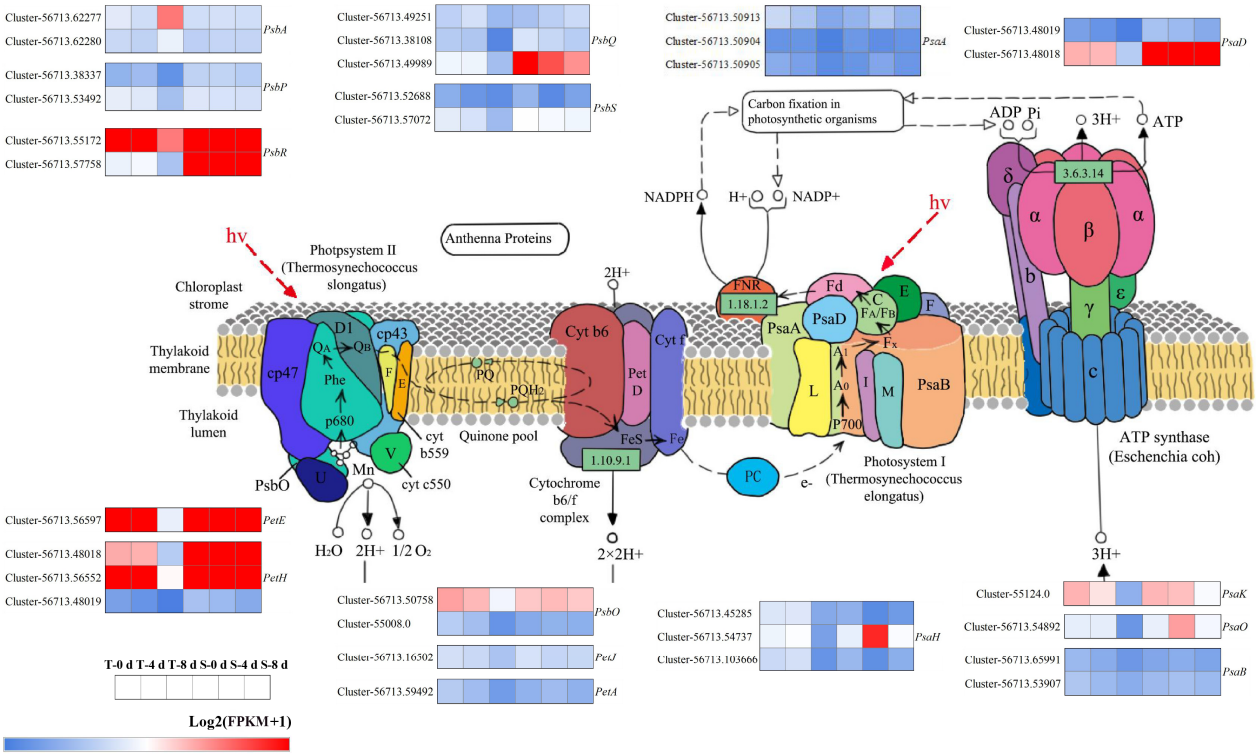


Figure 7. Analysis of photosynthetic pathways of DEGs under drought stress.

3.7. Transcription Factors Responding to Drought Stress

Transcription factors (TFs) are essential regulatory proteins that bind to cis-acting regulatory elements in target gene promoters, thereby modulating the expression of multiple genes [45]. In this study, a total of 565 TFs were identified (Figure 8A), including bHLH

(14%), WRKY (12.59%), bZIP (11.51%), MYB-related (10.43%), MYB (10.25%), C2H2 (5.93%), C2C2-GATA (5.22%), TCP (3.96%), E2F-DP (3.78%), HSF (3.23%), and others. Based on the GO annotation analysis, a total of 455 differentially expressed transcription factors (TFs) were identified (Table S4). Among these, we analyzed the expression levels of the top 10 TF families (Figure 8B), which included 66 basic helix–loop–helix (bHLH) factors, 69 WRKY domain-containing proteins, 31 basic leucine zipper (bZIP) factors, 55 MYB-related proteins, 56 MYB domain proteins, 8 C2H2 zinc finger proteins, 25 C2C2-GATA factors, 22 TCP family proteins, 7 E2F-DP heterodimers, and 17 heat shock factors (HSFs). Significant changes in the expression levels of these TF families were observed under different treatments. There were 27 and 41 downregulated *bHLHs* at T-4 d and T-8 d, and 27 and 35 downregulated *bHLHs* at S-4 d and S-8 d, respectively. The number of downregulated genes was higher than the number of genes upregulated genes, especially in the later period of treatment. Notably, *bHLH* genes, particularly *bHLH79* (Cluster-56713.42649), were downregulated by 0.74 and 3.02-fold in SKSZX and TRMG, respectively, while *bHLH30* (Cluster-58709.0) showed no significant changes. One-third of *bZIPs* were downregulated at T-4 d, T-8 d, S-4 d, and S-8 d. Additionally, the expression of *bZIP4* (Cluster-59385.0) and *bZIP44* (Cluster-56713.50670) was downregulated by 3.40- and 3.45-fold, respectively, under drought stress. MYB-related TFs were predominantly upregulated at T_4 d and T_8 d, while *MYBs* showed a contrasting trend. The number of downregulated *TCPs* at T-4 d and T-8 d was much higher than at S-4 d and S-8 d. The majority of HSFs were upregulated, with 9, 9, 11, and 13 HSFs upregulated at T-4 d, T-8 d, S-4 d, and S-8 d, respectively; 35 and 25 WRKYs were downregulated at T-4 d and S-4 d, and most of them were upregulated in the later stages of drought stress. *WRKY72* (Cluster-56713.97830), *WRKY24* (Cluster-56713.48840), and *WRKY23* (Cluster-56713.88836) showed the highest expression at 8 d, while *WRKY75* (Cluster-56713.93898), *WRKY2* (Cluster-56713.76165), and *WRKY48* (Cluster-56713.59956) displayed a decreased expression during the early drought stages but peaked later.

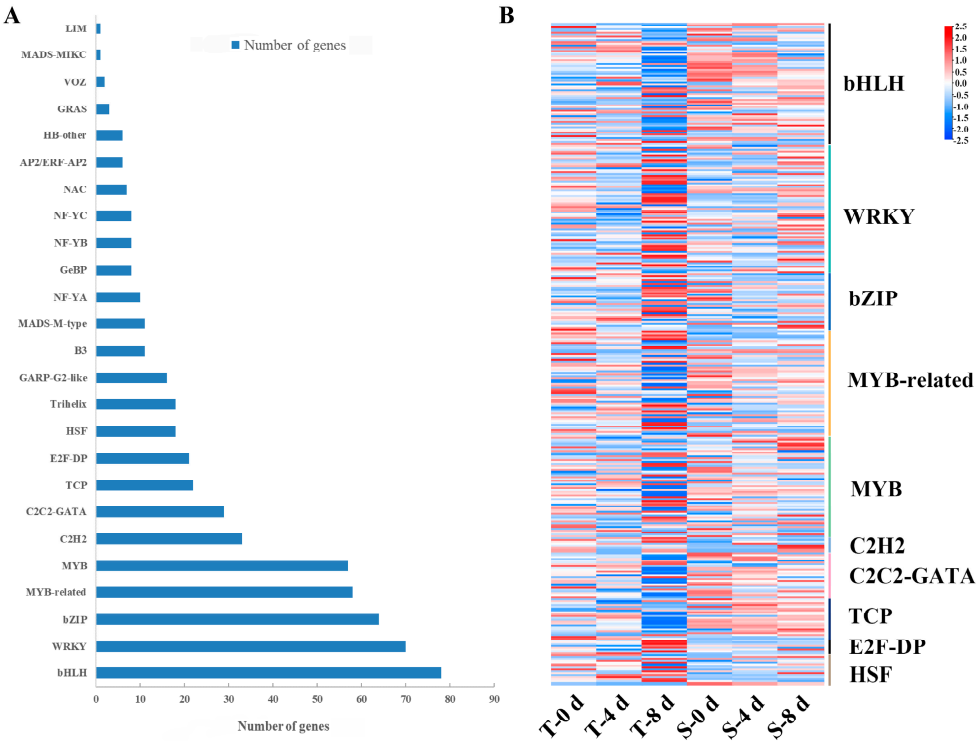


Figure 8. Analysis of transcription factors under drought stress. (**A**) Classification of transcription factor families. (**B**) Heat maps of the top ten differential TFs.

3.8. Validation of the DEGs by qRT-PCR

To confirm the accuracy and reproducibility of RNA-seq data, nine drought stress-related genes were selected for a transcript abundance analysis using qRT-PCR (Figure 9). The relative expression levels of these genes were compared with their FPKM values obtained from the transcriptional data. The results indicated that the expression profiles detected by qRT-PCR were consistent with those from RNA-seq, thereby confirming the reliability of the transcriptome data through the congruence between the RNA-seq and qRT-PCR results.

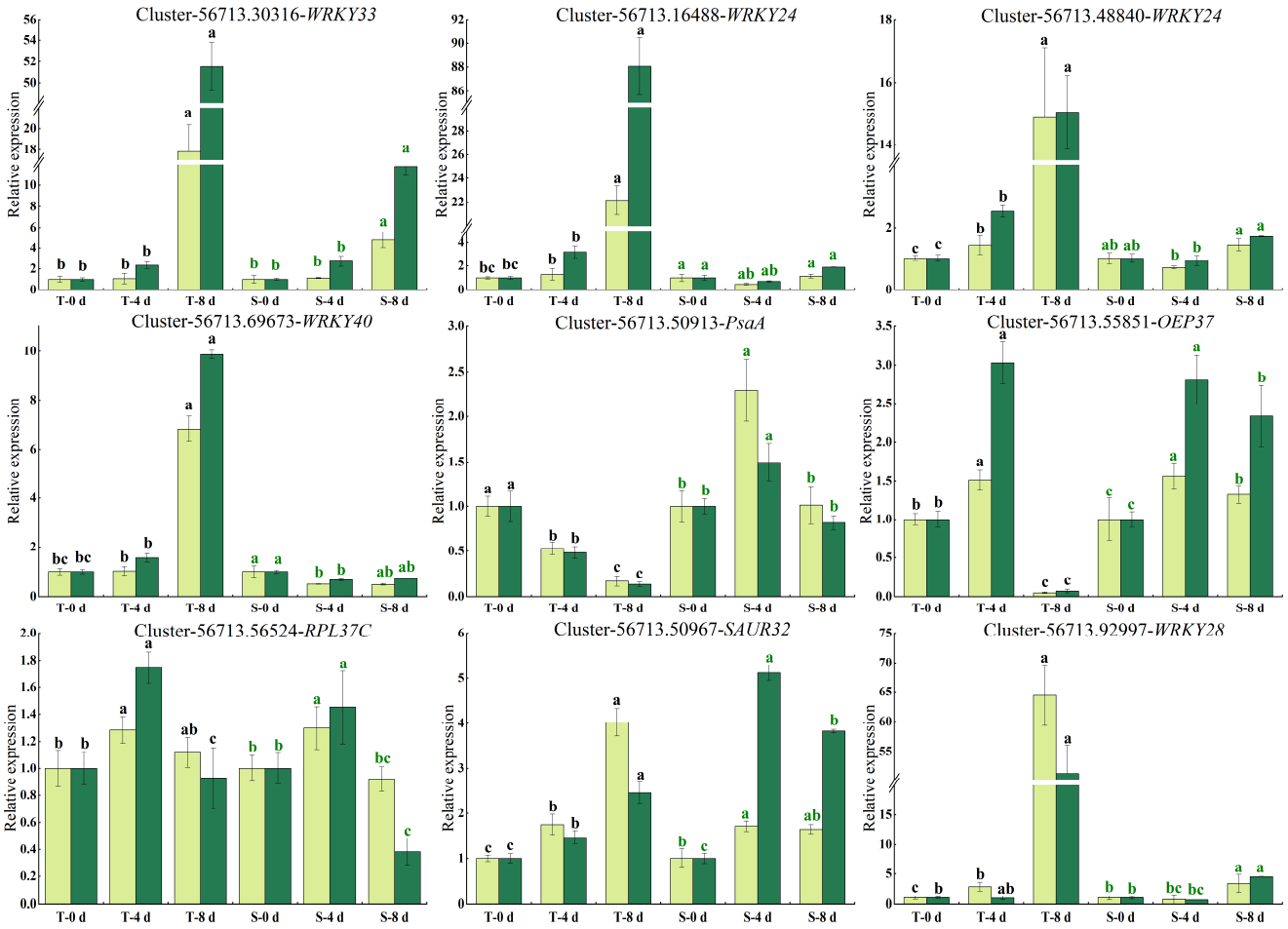


Figure 9. qRT-PCR analysis of nine differentially expressed genes under drought stress. Values indicate the mean ± standard error; the expression of genes at 0 d is normalized to "1"; and one-way ANOVA Duncan test was conducted ($p < 0.05$), with different lowercase letters representing significant differences. Note: Dark green denotes results from qRT-PCR validation, whereas light green corresponds to transcriptomic sequencing data derived from RNA-seq analysis.

4. Discussion

Rhododendron, one of China's ten most iconic traditional flowers, is renowned for its ornamental value and widespread use in landscaping. However, its ability to withstand drought stress remains limited. Understanding its genetic diversity is crucial for developing drought-resistant cultivars [46]. In this study, we examined the physiological and molecular responses of two *Rhododendron* cultivars, SKSZX and TRMG, to drought stress, providing valuable insights into selecting drought-tolerant cultivars.

Physiological analyses revealed marked differences in the responses of SKSZX and TRMG to drought stress. Leaf rolling is a common passive response to water scarcity, involving the adjustment of turgor pressure to delay leaf death by reducing the leaf surface area, water consumption, and evaporation [47]. TRMG exhibited more severe leaf curl-

ing, wilting, and drooping compared to SKSZX as the drought stress duration increased (Figure S1). SKSZX exhibited only mild leaf curling at the late drought stage (10 d), likely due to its prioritized resource allocation to stress-tolerant traits (e.g., lignin deposition and stomatal closure). In contrast, TRMG showed severe leaf wilting and drooping at as early as 4 d of drought, potentially reflecting its strategy to maximize the photosynthetic efficiency and growth rate at the expense of phenotypic plasticity under stress. A large number of studies have shown that, under drought stress, *Rhododendrons* usually exhibit symptoms such as new leaves curling up, drooping and wilting, and yellowing and withering of the leaf tips and edges. Moreover, as drought stress intensifies, the damage becomes more severe, and, in severe cases, the entire plant may die [48].

Chlorophyll fluorescence kinetic parameters can effectively reflect the intrinsic changes in light energy absorption and transfer during plant photosynthesis under stress conditions [49]. In this study, drought stress led to altered OJIP transients in both cultivars (Figure 1). Prolonged drought stress reduced the fluorescence peak (F_P), decreased the amplitude of the I-P phase, and increased the amplitude of the J-step and the J-I phase. These changes are consistent with those observed in maize and other species under similar conditions [50–52]. The decline in F_P may be attributed to several factors, including the increased non-radiative dissipation of PSII antenna chlorophylls, reduced PSII antenna size, a decreased number of functional PSII reaction centers (RCs), damage to the PSI acceptor side, and chlorophyll protein degradation [43,53–56]. Drought stress altered the redox status of PSI, as indicated by the reduction in the I-P phase [30,57]. Additionally, the increase in the J-I phase suggests reduced active PQ molecules that are typically reduced by each active PSII RC [55]. Concurrently, associated JIP-test parameters divulged varied impacts on the entire electron transport chain (ETC) of the photosynthetic system in two *Rhododendron* cultivars. The parameter δR_O reflects the electron transfer efficiency from the photosynthetic reduction system to the PSI acceptor side. As a light-absorption-based photosynthetic performance index (PI_{ABS}), it serves as a key indicator for assessing plant photosynthetic activity. In this study, PI_{TOTAL} was used as the integrated photosynthetic performance index, consistent with previous research [58]. After 10 d of drought stress, φE_O significantly decreased by 17.7% and 39.6% in SKSZX and TRMG, respectively (Figure 3C), while ψ_O decreased by 18.0% and 29.9%, respectively (Figure 3D). These findings suggest that the photosynthetic electron transfer beyond Q_A was compromised [59]. δR_O, a measure of relative PSI changes, showed smaller declines after 10 d of drought treatment.

The MR dynamics reflect changes in the redox state of PC and P700 [60]. The lowest points of MR/MR_O transients for SKSZX and TRMG were observed in the later stages of drought treatment (Figure 2A,D). DF, being highly sensitive to photosynthetic activity, demonstrated a marked reduction in induction kinetics as drought stress intensified (Figure 2B,E), and the DF decay curve showed a significant attenuation in the late stage of drought stress (Figure 2C,F). These results indicate that drought stress impaired the reverse electron transfer and reduced charge recombination, consequently hindering the regeneration of PSII antenna chlorophylls upon excitation [41]. Previous studies have shown that the I_1 peak corresponds to the transmembrane electric potential and the accumulation of reaction centers with a semi-reduced $Z^+P680QAQB^-$, whereas the I_2 peak is associated with an increase in the $Z^+P680QA^-QB^-$ state during the reduction in the PQ pool [50,61]. The decreased amplitudes of both I_1 and I_2 in the DF induction curve suggests that severe drought stress disrupted both the acceptor-side and donor-side electron transfer capacity of PSII, thereby reducing the net photosynthetic rate and the plants' ability to adapt to environmental stress [44,62]. Meanwhile, TRMG exhibited more rapid and pronounced declines in these parameters than SKSZX, suggesting that TRMG was more severely affected by drought stress.

The transcriptomic analysis is a powerful tool for identifying the genes, pathways, and processes associated with plant stress tolerance. In this study, a total of 1710 and 8144 DEGs were identified in the S-4 d and S-8 d treatments, respectively, while 3283 and 19,643 DEGs were detected in the T-4 d and T-8 d treatments (Figure 4A). Interestingly, the number of downregulated DEGs in TRMG at T-8 d was higher than that of upregulated DEGs, while the reverse pattern was observed in SKSZX at S-8 d. This contrasts with the findings in *Medicago sativa*, where drought-tolerant genotypes exhibited the earlier and sustained upregulation of stress-responsive genes [46].

To further explore the functional implications of the DEGs, we performed a KEGG enrichment analysis. In the seven comparison groups, upregulated genes were enriched in 38 KEGG pathways, and downregulated genes in 34 pathways (Figure 5A,B). This suggests upregulated genes are involved in a broader range of processes. The upregulated genes are linked to key metabolic and signaling pathways like "Tyrosine metabolism", "Starch and sucrose metabolism", and "Plant hormone signal transduction", which are vital for stress responses and growth. Meanwhile, downregulated genes are connected to pathways such as "Galactose metabolism" and "Glycerophospholipid metabolism", indicating specific metabolic adjustments. The difference in pathway numbers shows the plant may activate more diverse pathways to handle stress while downregulating select processes. The KEGG pathway enrichment analysis revealed that pathways such as "Tyrosine metabolism", "Starch and sucrose metabolism", and "Plant hormone signal transduction" were significantly enriched in upregulated DEGs (Figure 5C,E). This suggests these pathways are considerably influenced by the treatment conditions. Similarly, pathways like "Galactose metabolism" and "Glycerophospholipid metabolism" were notably enriched in downregulated DEGs (Figure 5D,F). As is well-known, photosynthesis plays a critical role in plant growth and development [63]. The enrichment in phenylpropanoid biosynthesis and photosynthesis pathways mirrors reports in soybean and *Setaria italica*, where phenylpropanoids conferred oxidative protection under drought stress [64,65]. The aforementioned results indicated that metabolic processes and photosynthesis likely play dominant roles during the middle and late stages of drought treatment, and the SKSZX and TRMG cultivars may respond to drought stress through distinct biological processes.

Plant hormones are key regulators of various signal transduction pathways during abiotic stress responses. Drought stress significantly influences endogenous hormone synthesis and signal transduction in plants [66]. In this study, we observed significant changes in gene expression related to plant hormone signaling pathways following drought treatment, indicating that plant hormones may play pivotal roles in *Rhododendron*'s response to drought stress. Auxin is essential for plant growth, development, and response to various abiotic stresses [67]. As auxin coreceptors and transcriptional suppressors, AUX/IAA proteins are critical components of auxin signal transduction [64]. In sorghum, *SbIAA1* is positively induced by drought treatment [68]. In rice, the overexpression of *OsIAA6* enhances drought resistance [69]. As an early auxin-response gene, *SAUR39* inhibits root and leaf growth while increasing the sugar, abscisic acid, and anthocyanin content, thereby altering rice resistance [70]. The post-transcriptional regulation of *ARF* expression by miR160 and miR165/166 improves drought tolerance in *Arabidopsis thaliana* [71]. GH3 plays an important role in regulating hormonal homeostasis and facilitating rapid responses to abiotic stresses. Under natural conditions, the expression level of *SbGH3* was relatively low, but it was significantly upregulated under drought stress [72]. It is noted that, compared with SKSZX, two *AUX/IAA* genes were upregulated and four *AUX/IAA* genes were downregulated under 4 d and 8 d treatments. The expression of four genes encoding *ARF* was inhibited during the whole process of drought stress. One upregulated gene encoding *GH3* and two upregulated genes encoding *SAUR* were found after SKSZX treatment for

4 d. Two downregulated genes encoding *GH3* and three downregulated genes encoding *SAUR* were found after SKSZX treatment for 8 d (Figure 6A). Additionally, ABA, a crucial endogenous signaling molecule, was involved in the drought response [73]. Drought stress leads to a significant increase in plants' ABA levels, accompanied by adaptive physiological responses. In TRMG, four genes encoding *PP2C* were downregulated at 4 d and 8 d treatments. Notably, two *SnRK2* genes (Cluster-56713.52170 and Cluster-56713.46758) were upregulated in SKSZX but downregulated in TRMG at 8 d (Figure 6B). These genes, along with ABA-responsive genes (Cluster-56713.71630 and Cluster-56713.71875), are proposed as priority candidates for future functional validation due to their central roles in ABA signaling and drought tolerance. It is widely acknowledged that photosynthesis is one of the primary processes that drive plant growth and development [63]. In this study, we found that many core components of PSI and PSII were markedly downregulated in TRMG under drought, while SKSZX showed a more stable expression. For example, PSI-related genes like *PsaA*, *PsaB*, and *PsaD* were substantially downregulated in TRMG, whereas SKSZX exhibited much milder suppression. Similarly, PSII-related genes also showed a similar downregulation pattern in TRMG, while SKSZX maintained a relatively stable expression or even a slight upregulation. Notably, the downregulation of PSI/PSII genes in TRMG (Figure 7) parallels the photosynthetic inhibition in drought-stressed wheat [55], while SKSZX's resilience may stem from the maintained expression of *PetE* and *PsbO*, akin to the osmoprotective strategies in *Scutellaria baicalensis* [74].

In this study, a large number of TFs, including bHLH, WRKY, bZIP, MYB-related, MYB, C2H2, C2C2-GATA, TCP, E2F-DP, and HSF, were obtained by transcriptome sequencing. Several studies have shown that *bHLHs* actively participate in the regulation of plant stress resistance [75,76]. More downregulated bHLHs were found in TRMG than in SKSZX. In SKSZX and TRMG, *bHLH79* downregulated by 0.74- and 3.02-fold, respectively. Nevertheless, *bHLH30* has no appreciable change in gene expression in the whole stage of treatment. In rice, *bZIP71* was significantly enriched after PEG treatment [77]. In *Setaria italica*, the upregulation of *SibZIP12* and *SibZIP72* was found to be associated with the response to root drought stress [65]. Approximately one-third of *bZIPs* were downregulated in both cultivars, such as *bZIP4* and *bZIP44*, which exhibited the most significant downregulation, with reductions of 3.40- and 3.45-fold, respectively. In *Scutellaria baicalensis*, *SbMYB8* enhanced the drought stress tolerance of transgenic plants by regulating flavonoid biosynthesis [74]. The expression of *ZmMYB3R* improved the drought and salt stress tolerance in transgenic plants [78], and *PtrMYB94* has also been reported to work synergistically with ABA signaling to improve drought tolerance [79]. At T-4 d and T-8 d, the majority of *MYBs* exhibited downregulation, whereas the opposite pattern was observed at S-4 d and S-8 d. Numerous studies have shown that *WRKYs* have important biological functions in response to various biotic and abiotic stresses [80]. For instance, the overexpression of *VaWRKY14* enhanced drought tolerance in transgenic *Arabidopsis* [81]. However, some WRKYs can act as negative regulators of abiotic stresses in plants. For example, *PagWRKY75* was downregulated in the early stages of osmotic stress, and transgenic poplar plants were more sensitive to osmotic stress [82]. In this study, most of the *WRKYs* were upregulated during the later stages of drought stress. *WRKY72*, *WRKY24*, and *WRKY23* reached the highest expression level at 8 d. *WRKY75*, *WRKY2*, and *WRKY48* were initially downregulated but subsequently reached peak expression levels in the later periods of drought stress.

5. Conclusions

In conclusion, we compared and characterized the physiological and molecular responses of two *Rhododendron* cultivars, SKSZX and TRMG, to drought stress. By simultaneously measuring the kinetics of PF, DF, and MR in the photosystems of both cultivars, we

observed substantial alterations in the photosynthetic electron transport chain. Drought stress disrupted several key sites within the chain, particularly affecting the PSI acceptor-side electron transporters and reducing the electron flow from Q_A to Q_B. As a result, both PSI and PSII activities were compromised, with TRMG exhibiting more pronounced reductions compared to SKSZX, highlighting cultivar-specific drought responses. A transcriptome analysis revealed a greater number of DEGs in TRMG, suggesting that SKSZX maintained a more stable gene expression and displayed superior drought tolerance. These DEGs were primarily enriched in pathways related to phenylpropanoid biosynthesis, plant hormone signaling, and photosynthesis, indicating their potential roles in enhancing drought tolerance. These findings offer valuable insights into the molecular mechanisms underpinning drought resistance in *Rhododendron* and provide a theoretical foundation for the development of drought-resistant cultivars.

Supplementary Materials: The following supporting information can be downloaded at: https://www.mdpi.com/article/10.3390/agronomy15061278/s1, Figure S1: Drought-stress-induced phenotypic responses in two Rhododendron species; Figure S2: Integrated analysis of gene expression data: (A) Cluster heatmap of DEGs; (B) Correlation heatmap; (C) Principal component analysis (PCA) of samples; Table S1: Primer sequences for qRT-PCR validation of DEGs; Table S2: Top 20 significantly enriched GO terms in up- and downregulated differentially expressed genes (DEGs); Table S3: KEGG pathway enrichment analysis of differentially expressed genes (DEGs) across treatment groups; Table S4: Information related to the GO annotation of transcription factors.

Author Contributions: Conceptualization, X.L.; methodology, X.L. and Z.W.; software, Z.W.; validation, Z.W. and X.Z.; investigation, X.L., Z.W., and Y.W.; resources, X.Z.; data curation, S.J.; writing—original draft preparation, X.L. and Z.W.; writing—review and editing, S.J. and Z.W.; supervision, Y.W.; project administration, S.J.; funding acquisition, S.J. All authors have read and agreed to the published version of the manuscript.

Funding: This research was funded by the National Key Research and Development Project (2019YFE0118900), National Natural Science Foundation of China (31971641), and Zhejiang Province Forestry Special Plan Project (20250011).

Data Availability Statement: All reads used in this study were deposited in the NCBI Sequence Read Archive under accession number PRJNA1184443.

Conflicts of Interest: The authors declare no conflicts of interest.

References

1. Song, M.B.; Mu, L.Q. *Rhododendron* plant resources and landscape application. *Spec. Econ. Anim. Plants* **2022**, *25*, 103–104.
2. Scheiber, S.M.; Jarret, R.L.; Robacker, C.D.; Newman, M. Genetic relationships within *Rhododendron* L. section Pentanthera G. Don based on sequences of the internal transcribed spacer (ITS) region. *Sci. Hortic.* **2000**, *85*, 123–135. [CrossRef]
3. Popescu, R.; Kopp, B. The genus Rhododendron: An ethnopharmacological and toxicological review. *J. Ethnopharmacol.* **2013**, *147*, 42–62. [CrossRef] [PubMed]
4. Gautam, V.; Kohli, S.K.; Kapoor, D.; Bakshi, P.; Ahmad, P. Stress Protective Effect of *Rhododendron arboreum* Leaves (MEL) on Chromium-Treated Vigna radiata Plants. *J. Plant Growth Regul.* **2021**, *40*, 423–435. [CrossRef]
5. Wang, X.Q.; Huang, Y.; Long, C.L. Cross-amplification and characterization of microsatellite loci for the genus Rhododendron. *Hortscience* **2010**, *45*, 1394–1397. [CrossRef]
6. Wang, S.; Li, Z.; Jin, W.; Fang, Y.; Yang, Q.; Xiang, J. Transcriptome analysis and identification of genes associated with flower development in Rhododendron *pulchrum* Sweet (Ericaceae). *Gene* **2018**, *679*, 108–118. [CrossRef] [PubMed]
7. De Riek, J. *Ornamental Crops*; Springer: Cham, Switzerland, 2018; Volume 11, pp. 237–271.
8. Xie, W.J. Thewell-established industrial system of Belgian Azaleas. *China Flowers Hortic.* **2015**, *5*, 56–57.
9. Li, X.C. Greenhouse cultivation techniques of Belgian Azaleas. *Chin. Hortic. Abstr.* **2009**, *25*, 146–147.
10. Wang, Z.C. The Landscape Construction of *Rhododendron* Special Garden in National Forest Park of Hunan Dawei Mountain. Master's Thesis, Central South University of Forestry and Technology, Changsha, China, 2014.

11. Zhu, C.Y.; Yu, J.L.; Lv, M.; Zhu, J.J. Flowering characteristics and cultivation adaptability of 28 *Rhododendron* cultivars. *J. Agric.* **2015**, *5*, 82–86.
12. Zhou, L.L. Research on Plant Landscape of *Rhododendron*. Master's Thesis, Zhejiang A&F University, Hangzhou, China, 2013.
13. Zhou, W.W. Development status of Rhododendron industry in China. *China Flowers Hortic.* **2010**, *9*, 12–14.
14. Wu, H.; Yang, X.M.; Shao, H.M.; Wang, F. Germplasm resources base for *Rhododendron* horticulture: Status, problems and countermeasures. *Biodivers. Sci.* **2013**, *21*, 628–634.
15. Ou, J.; Chen, X. Resources and landscape application prospects of Subgen. Hymenanthes in Guizhou Province. *Jiangsu Agric. Sci.* **2012**, *40*, 200–203.
16. Sleumer, H. Ein system der gattung *Rhododendron* L. *Bot. Jahrb. Syst.* **1949**, *74*, 511–553.
17. Todaka, D.; Zhao, Y.; Yoshida, T.; Kudo, M.; Kidokoro, S.; Mizoi, J.; Kodaira, K.S.; Takebayashi, Y.; Kojima, M.; Sakakibara, H.; et al. Temporal and spatial changes in gene expression, metabolite accumulation and phytohormone content in rice seedlings grown under drought stress conditions. *Plant J.* **2017**, *90*, 61–78. [CrossRef] [PubMed]
18. Pan, J.; Li, Z.; Wang, Q.; Garrell, A.K.; Liu, M.; Guan, Y.; Zhou, W.; Liu, W. Comparative proteomic investigation of drought responses in foxtail millet. *BMC Plant Biol.* **2018**, *18*, 315. [CrossRef]
19. Xu, K.; Chen, S.; Li, T.; Ma, X.; Liang, X.; Ding, X.; Liu, H.; Luo, L. *OsGRAS23*, a rice GRAS transcription factor gene, is involved in drought stress response through regulating expression of stress-responsive genes. *BMC Plant Biol.* **2015**, *15*, 141. [CrossRef]
20. Chen, G.; Wang, Y.; Wang, X.; Yang, Q.; Quan, X.; Zeng, J.; Dai, F.; Zeng, F.; Wu, F.; Zhang, G.; et al. Leaf epidermis transcriptome reveals drought-Induced hormonal signaling for stomatal regulation in wild barley. *Plant Growth Regul.* **2018**, *87*, 39–54. [CrossRef]
21. Zhang, X.; Lei, L.; Lai, J.; Zhao, H.; Song, W. Effects of drought stress and water recovery on physiological responses and gene expression in maize seedlings. *BMC Plant Biol.* **2018**, *18*, 68. [CrossRef]
22. Shinozaki, K.; Yamaguchi-Shinozaki, K. Gene networks involved in drought stress response and tolerance. *J. Exp. Bot.* **2007**, *58*, 221–227. [CrossRef]
23. Vivekanandan, M. Drought-induced responses of photosynthesis and antioxidant metabolism in higher plants. *J. Plant Physiol.* **2004**, *161*, 1189–1202.
24. Zelitch, I. The close relationship between net photosynthesis and crop yield. *Bioscience* **1982**, *32*, 796–802. [CrossRef]
25. Strasser, R.J.; Srivastava, A.; Govindjee. Polyphasic chlorophyll a fluorescence transient in plants and cyanobacteria. *Photochem. Photobiol.* **1995**, *61*, 32–42. [CrossRef]
26. Strasser, R.J.; Srivastava, A.; Tsimilli-Michael, M. Analysis of the chlorophyll a fluorescence transient. Chlorophyll fluorescence: A signature of photosynthesis. In *Chlorophyll a Fluorescence: A Signature of Photosynthesis*; Papageorgiou, G.C., Govindjee, Eds.; Advances in Photosynthesis and Respiration Series; Springer: Dordrecht, The Netherlands, 2004; Volume 19, pp. 321–362.
27. Schansker, G.; Tóth, S.Z.; Strasser, R.J. Methylviologen and dibromothymoquinone treatments of pea leaves reveal the role of photosystem I in the Chl a fluorescence rise OJIP. *Biochim. Biophys. Acta* **1706**, *2005*, 250–261. [CrossRef] [PubMed]
28. Stirbet, A.; Govindjee. Chlorophyll a fluorescence induction: A personal perspective of the thermal phase, the J-I-P rise. *Photosynth. Res.* **2012**, *113*, 15–61. [CrossRef]
29. Strehler, B.L.; Arnold, W. Light production by green plants. *J. Gen. Physiol.* **1951**, *34*, 809–820. [CrossRef]
30. Schansker, G.; Srivastava, A.; Govindjee; Strasser, R.J. Characterization of the 820-nm transmission signal paralleling the chlorophyll a fluorescence rise (OJIP) in pea leaves. *Funct. Plant Biol.* **2003**, *30*, 785–796.
31. Chen, L.; Yu, S.; Li, S.; Zhang, L.; Zou, C.; Yu, D. The role of WRKY transcription factors in plant abiotic stresses. *Biochim. Biophys. Acta* **2012**, *1819*, 120–128. [CrossRef]
32. Irigoyen, J.J.; Emerich, D.W.; Sánchez-Díaz, M. Alfalfa leaf senescence induced by drought stress: Photosynthesis, hydrogen peroxide metabolism, lipid peroxidation and ethylene evolution. *Physiol. Plant.* **2010**, *84*, 67–72. [CrossRef]
33. Shen, B.; Jensen, R.G.; Bohnert, H.J. Increased resistance to oxidative stress in transgenic plants by targeting mannitol biosynthesis to chloroplasts. *Plant Physiol.* **1997**, *113*, 1177–1183. [CrossRef]
34. Shinozaki, K.; Yamaguchi-Shinozaki, K. Gene Expression and signal transduction in water-stress response. *Plant Physiol.* **1997**, *115*, 327–334. [CrossRef]
35. Liu, X.; Zhang, R.; Ou, H.; Gui, Y.; Wei, J.; Zhou, H.; Tan, H.; Li, Y. Comprehensive transcriptome analysis reveals genes in response to water deficit in the leaves of *Saccharum narenga* (Nees ex Steud.) hack. *BMC Plant Biol.* **2018**, *18*, 250. [CrossRef] [PubMed]
36. Ji, T.; Li, S.; Li, L.; Huang, M.; Wang, X.; Wei, M.; Shi, Q.; Li, Y.; Gong, B.; Yang, F. Cucumber *Phospholipase* D alpha gene overexpression in tobacco enhanced drought stress tolerance by regulating stomatal closure and lipid peroxidation. *BMC Plant Biol.* **2018**, *18*, 355. [CrossRef] [PubMed]
37. Hrdlickova, R.; Toloue, M.; Tian, B. RNA-Seq methods for transcriptome analysis. *Wiley Interdiscip. Rev. RNA* **2017**, *8*, e1364. [CrossRef] [PubMed]

38. Li, X.; Bai, W.; Yang, Q.; Yin, B.; Zhang, Z.; Zhao, B.; Kuang, T.; Zhang, Y.; Zhang, D. The extremotolerant desert moss *Syntrichia caninervis* is a promising pioneer plant for colonizing extraterrestrial environments. *Innovation* **2024**, *5*, 100657. [CrossRef]
39. Haas, B.; Papanicolaou, A.; Yassour, M.; Grabherr, M.; Blood, P.; Bowden, J.; Couger, M.; Eccles, D.; Li, B.; Lieber, M.; et al. De novo transcript sequence reconstruction from RNA-seq using the Trinity platform for reference generation and analysis. *Nat. Protoc.* **2013**, *8*, 1494–1512. [CrossRef]
40. Marchant, A.; Mougel, F.; Mendonça, V.; Quartier, M.; Jacquin-Joly, E.; Rosa, J.; Petit, E.; Harry, M. Comparing de novo and reference-based transcriptome assembly strategies by applying them to the blood-sucking bug *Rhodnius prolixus*. *Insect Biochem. Mol. Biol.* **2016**, *69*, 25–33. [CrossRef]
41. Strasser, R.J.; Tsimilli-Michael, M.; Qiang, S.; Goltsev, V. Simultaneous in vivo recording of prompt and delayed fluorescence and 820-nm reflection changes during drying and after rehydration of the resurrection plant *Haberlea rhodopensis*. *Biochim. Biophys. Acta* **2010**, *1797*, 1313–1326. [CrossRef]
42. Strasser, R.J.; Tsimilli-Michael, M. Experimental approach to estimate in vivo the balance of the mechanisms for performance of light reactions, dark reactions, energetic cooperativity, non-Q(A)-and non-Q(B)-reducing and non-oxygen-evolving PSII centers. *Acta Physiol. Plant.* **2004**, *26*, 94.
43. Oukarroum, A.; Goltsev, V.; Strasser, R.J. Temperature effects on pea plants probed by simultaneous measurements of the kinetics of prompt fluorescence, delayed fluorescence and modulated 820 nm reflection. *PLoS ONE* **2013**, *8*, e59433. [CrossRef]
44. Gao, J.; Li, P.; Ma, F.; Goltsev, V. Photosynthetic performance during leaf expansion in *Malus micromalus* probed by chlorophyll a fluorescence and modulated 820 nm reflection. *J. Photochem. Photobiol. B* **2014**, *137*, 144–150. [CrossRef]
45. Dhriti, S.; Ashverya, L. Transcriptional regulation of drought response: A tortuous network of transcriptional factors. *Front. Plant Sci.* **2015**, *6*, 895.
46. Lei, Y.T.; Xu, Y.X.; Hettenhausen, C.; Lu, C.K.; Shen, G.J.; Zhang, C.P.; Li, J.; Song, J.; Lin, H.H.; Wu, J.Q. Comparative analysis of alfalfa (*Medicago sativa* L.) leaf transcriptomes reveals genotype-specific salt tolerance mechanisms. *BMC Plant Biol.* **2018**, *18*, 35. [CrossRef] [PubMed]
47. Hsiao, T.C.; O'Toole, J.C.; Yambao, E.B.; Turner, N.C. Influence of osmotic adjustment on leaf rolling and tissue death in rice (*Oryza sativa* L.). *Plant Physiol.* **1984**, *75*, 338–341. [CrossRef] [PubMed]
48. Zheng, Y.; Chen, Q.X. Evalution of drought resistance of six *Rhododendron* varities. *Jiangsu Agric. Sci.* **2019**, *47*, 163–167.
49. Wen, G.S.; Tian, H.T.; Zhang, M.R.; Jiang, W.W. Application of chlorophyll fluorescence Analysis in Forest Tree Cultivation. *J. Appl. Ecol.* **2006**, *17*, 1973–1977.
50. Oukarroum, A.; Schansker, G.; Strasser, R.J. Drought stress effects on photosystem I content and photosystem II thermotolerance analyzed using Chl a fluorescence kinetics in barley varieties differing in their drought tolerance. *Physiol. Plant.* **2010**, *137*, 188–199. [CrossRef]
51. Oukarroum, A.; Gharous, M.E.; Goltsev, V. Desiccation-induced changes of photosynthetic transport in *Parmelina tiliacea*, (Hoffm.) Ach. Analysed by simultaneous measurements of the kinetics of prompt fluorescence, delayed fluorescence and modulated 820 nm reflection. *J. Lumin.* **2018**, *198*, 302–308. [CrossRef]
52. Zong, Y.Z.; Wang, W.F.; Xue, Q.W. Interactive effects of elevated CO_2 and drought on photosynthetic capacity and PSII performance in maize. *Photosynthetica* **2014**, *52*, 63–70. [CrossRef]
53. Oukarroum, A.; Bussotti, F.; Goltsev, V.; Kalaji, H.M. Correlation between reactive oxygen species production and photochemistry of photosystems I and II in *Lemna gibba* L. plants under salt stress. *Environ. Exp. Bot.* **2015**, *109*, 80–88. [CrossRef]
54. Oukarroum, A.; Gharous, M.E.; Goltsev, V.; Strasser, R.J. Delayed fluorescence emission as a probe for the response of photosynthetic organisms to high temperature exposure: A comparative study. *J. Lumin.* **2016**, *180*, 321–327. [CrossRef]
55. Paunov, M.; Koleva, L.; Vassilev, A.; Vangronsveld, J.; Goltsev, V. Effects of different metals on photosynthesis: Cadmium and zinc affect chlorophyll fluorescence in durum wheat. *Int. J. Mol. Sci.* **2018**, *19*, 787. [CrossRef] [PubMed]
56. Gao, Y.; Liu, W.; Wang, X. Comparative phytotoxicity of usnic acid, salicylic acid, cinnamic acid and benzoic acid on photosynthetic apparatus of Chlamydomonas reinhardtii. *Plant Physiol. Biochem.* **2018**, *128*, 1. [CrossRef] [PubMed]
57. Dąbrowski, P.; Baczewska, A.H.; Pawluśkiewicz, B. Prompt chlorophyll a fluorescence as a rapid tool for diagnostic changes in PSII structure inhibited by salt stress in Perennial ryegrass. *J. Photochem. Photobiol. B* **2016**, *157*, 22–31. [CrossRef] [PubMed]
58. Shu, P.Z.; Gong, X.F.; Du, Y.L.; Han, Y.N.; Jin, S.H.; Wang, Z.X.; Qian, P.H.; Li, X.Q. Effects of simulated acid rain on photosynthesis in *Pinus massoniana* and *Cunninghamia lanceolatain* terms of prompt fluorescence, delayed fluorescence, and modulated reflection at 820 nm. *Plants* **2024**, *13*, 622. [CrossRef]
59. Sheng, Q.; Chen, S.; Strasser, R.O.J.; Yang, J.; Zhang, M. Classifcation and characteristics of heat tolerance in *Ageratina adenophora* populations using fast chlorophyll a fuorescence rise O–J–I–P. *Environ. Exp. Bot.* **2016**, *122*, 126–140.
60. Guo, Y.; Lu, Y.; Goltsev, V.; Strasser, R.J.; Kalaji, H.M.; Wang, H.; Wang, X.; Chen, S.; Qiang, S. Comparative efect of tenuazonic acid, diuron, bentazone, dibromothymoquinone and methyl viologen on the kinetics of Chl a fuorescence rise OJIP and the MR820 signal. *Plant Physiol. Biochem.* **2020**, *156*, 39–48. [CrossRef]

61. Goltsev, V.; Chernev, P.; Zaharieva, I.; Lambrev, P.; Strasser, R.J. Kinetics of delayed chlorophyll a fluorescence registered in milliseconds time range. *Photosynth. Res.* **2005**, *84*, 209–215. [CrossRef]
62. Duan, Y.; Zhang, M.; Gao, J. Thermotolerance of apple tree leaves probed by chlorophyll a fluorescence and modulated 820 nm reflection during seasonal shift. *J. Photochem. Photobiol. B* **2015**, *152*, 347–356. [CrossRef]
63. Wit, M.; Galvão, V.; Fankhauser, C. Light−Mediated Hormonal Regulation of Plant Growth and Development. Annu. *Rev. Plant Biol.* **2016**, *67*, 513–537. [CrossRef]
64. Xuan, H.D.; Huang, Y.Z.; Zhou, L.; Deng, S.S.; Wang, C.C.; Xu, J.Y.; Wang, H.T.; Zhao, J.M.; Guo, N.; Xing, H. Key soybean seedlings drought-responsive genes and pathways revealed by comparative transcriptome analyses of two cultivars. *Int. J. Mol. Sci.* **2022**, *23*, 2893. [CrossRef]
65. Lu, P.; Wu, Y.M.; Wu, Q.Q.; Li, X.Y. Genome-wide identification and bioinformatics analysis of *Setaria italica* bZIP transcription factor family. *J. Shanxi Agric. Sci.* **2020**, *48*, 1361–1370+1430.
66. Vishwakarma, K.; Upadhyay, N.; Kumar, N.; Yadav, G.; Singh, J.; Mishra, R.K.; Kumar, V.; Verma, R.; Upadhyay, R.G.; Pandey, M.; et al. Abscisic acid signaling and abiotic stress tolerance in plants: A review on current knowledge and future prospects. *Front. Plant Sci.* **2017**, *8*, 161. [CrossRef] [PubMed]
67. Singh, V.P.; Prasad, S.M.; Munné-Bosch, S.; Müller, M. Phytohormones and the regulation of stress tolerance in plants: Current status and future directions. *Front. Plant Sci.* **2017**, *8*, 1871. [CrossRef] [PubMed]
68. Wang, S.K.; Bai, Y.H.; Shen, C.J.; Wu, Y.R.; Zhang, S.N.; Jiang, D.A.; Guilfoyle, T.J.; Chen, M.; Qi, Y.H. Auxin-related gene families in abiotic stress response in Sorghum bicolor. *Funct. Integr. Genom.* **2010**, *10*, 533–546. [CrossRef]
69. Jung, H.; Lee, D.K.; Do Choi, Y.; Kim, J.K. OsIAA6, a member of the rice Aux/IAA gene family, is involved in drought tolerance and tiller outgrowth. *Plant Sci.* **2015**, *236*, 304–312. [CrossRef]
70. Kant, S.; Rothstein, S. Auxin-responsive SAUR39 gene modulates auxin level in rice. *Plant Signal. Behav.* **2009**, *4*, 1174–1175. [CrossRef]
71. Yang, T.X.; Wang, Y.Y.; Teotia, S.; Wang, Z.H.; Shi, C.N.; Sun, H.W.; Gu, Y.Y.; Zhang, Z.H.; Tang, G.L. The interaction between miR160 and miR165/166 in the control of leaf development and drought tolerance in *Arabidopsis*. *Sci. Rep.* **2019**, *9*, 2832. [CrossRef]
72. Chen, J.N.; Nolan, T.M.; Ye, H.X.; Zhang, M.C.; Tong, H.N.; Xin, P.Y.; Chu, J.F.; Chu, C.C.; Li, Z.H.; Yin, Y.H. Arabidopsis WRKY46, WRKY54, and WRKY70 transcription factors are involved in brassinosteroid-regulated plant growth and drought responses. *Plant Cell* **2017**, *29*, 1425–1439. [CrossRef]
73. Teng, K.; Li, J.; Liu, L.; Han, Y.; Du, Y.; Zhang, J.; Sun, H. Exogenous ABA induces drought tolerance in upland rice: The role of chloroplast and ABA biosynthesis-related gene expression on photosystem II during PEG stress. *Acta Physiol. Plant.* **2014**, *36*, 2219–2227. [CrossRef]
74. Yuan, Y.; Qi, L.J.; Yang, J.; Wu, C.; Liu, Y.J.; Huang, L.Q. A *Scutellaria baicalensis* R2R3-MYB gene, SbMYB8, regulates flavonoid biosynthesis and improves drought stress tolerance in transgenic tobacco. *Plant Cell Tissue Organ. Cult.* **2015**, *120*, 961–972. [CrossRef]
75. Liu, W.; Tai, H.; Li, S.; Gao, W.; Zhao, M.; Xie, C.; Li, W.-X. bHLH122 is important for drought and osmotic stress resistance in *Arabidopsis* and in the repression of ABA catabolism. *New Phytol.* **2014**, *201*, 1192–1204. [CrossRef] [PubMed]
76. Qiu, J.R.; Huang, Z.; Xiang, X.Y.; Xu, W.X.; Wang, J.T.; Chen, J.; Song, L.; Xiao, Y.; Li, X.; Ma, J.; et al. MfbHLH38, a *Myrothamnus flabellifolia* bHLH transcription factor, confers tolerance to drought and salinity stresses in *Arabidopsis*. *BMC Plant Biol.* **2020**, *20*, 542. [CrossRef] [PubMed]
77. Hao, C.; Wei, C.; Zhou, J.; Huang, H.; Chen, L.; Chen, H.; Xing, W.D. Basic leucine zipper transcription factor *OsbZIP16* positively regulates drought resistance in rice. *Plant Sci.* **2012**, *193/194*, 8–17.
78. Wu, J.D.; Jiang, Y.L.; Liang, Y.N.; Chen, L.; Chen, W.; Cheng, B. Expression of the maize MYB transcription factor ZmMYB3R enhances drought and salt stress tolerance in transgenic plants. *Plant Physiol. Biochem.* **2019**, *137*, 137179–137188. [CrossRef] [PubMed]
79. Fang, Q.; Wang, X.Q.; Wang, H.Y.; Tang, X.; Liu, C.; Yin, H.; Ye, S.; Jiang, Y.; Duan, Y.; Luo, K. The poplar R2R3 MYB transcription factor PtrMYB94 coordinates with abscisic acid signaling to improve drought tolerance in plants. *Tree Physiol.* **2020**, *40*, 46–59. [CrossRef]
80. Jiang, J.J.; Ma, S.H.; Ye, N.H.; Cao, J.S.; Zhang, J. WRKY transcription factors in plant responses to stresses. *J. Integr. Plant Biol.* **2017**, *59*, 86–101. [CrossRef]
81. Zhang, L.; Cheng, J.; Sun, X.; Zhao, T.; Li, M.; Wang, Q.; Li, S.; Xin, H. Overexpression of VaWRKY14 increases drought tolerance in *Arabidopsis* by modulating the expression of stress-related genes. *Plant Cell Rep.* **2018**, *37*, 1159–1172. [CrossRef]
82. Zhao, K.; Zhang, D.; Lv, K.; Zhang, X.; Jiang, T. Functional characterization of poplar WRKY75 in salt and osmotic tolerance. *Plant Sci.* **2019**, *289*, 110259. [CrossRef]

Disclaimer/Publisher's Note: The statements, opinions and data contained in all publications are solely those of the individual author(s) and contributor(s) and not of MDPI and/or the editor(s). MDPI and/or the editor(s) disclaim responsibility for any injury to people or property resulting from any ideas, methods, instructions or products referred to in the content.